



The Canadian Hydrological Model (CHM): A multi-scale, multi- extent, variable-complexity hydrological model -- Design and overview

Christopher B. Marsh^{1,2}

5 John W. Pomeroy^{1,2}

Howard S. Wheater^{2,1}

Affiliations: ¹ Centre for Hydrology, University of Saskatchewan, Canada.; ² Global Institute for Water Security, University of Saskatchewan, Canada

1 — Abstract

10 Despite debate in the rainfall-runoff hydrology literature about the merits of physics-based and spatially distributed models, substantial work in cold regions hydrology has shown improved predictive capacity by including physics-based process representations, relatively high-resolution semi- and fully-distributed discretizations, and use of physically identifiable parameters with limited calibration. While there is increasing motivation for modelling at hyper-resolution (< 1 km) and snow-drift resolving scales (~1 m to 100 m), the capabilities of existing cold-region hydrological models are computationally
15 limited at these scales.

Here, a new distributed model, the Canadian Hydrological Model (CHM), is presented. Although designed to be applied generally, it has a focus for application where cold-region processes play a role in hydrology. Key features include the ability to capture spatial heterogeneity in the surface discretization in an efficient manner; to include multiple process representations; to be able to change, remove, and decouple hydrological process algorithms; to work both at a point and
20 spatially distributed; the ability to scale to multiple spatial extents and scale; and to utilize a variety of forcing fields (boundary and initial conditions). This manuscript focuses on the overall model philosophy and design, and provides a number of cold-region-specific features and examples.

2 — Key points

- Novel unstructured mesh discretization allows for reduced computational cost while including spatial heterogeneity.
- 25 • Ability to modify structure and algorithms within a distributed framework allows for in-depth uncertainty testing.



- Flexible spatial and temporal scales, software abstraction, and robust pre- and post-processing routines allow for incorporating existing code, decreasing development effort.

3 — Introduction

Hydrological models are important tools for understanding past and predicting future hydrological events, informing infrastructure design, and evaluating anthropogenic impacts on natural systems (Freeze and Harlan, 1969). They are used for both research and operational water resource issues under contemporary and future climates (Debeer et al., 2015; Milly et al., 2008; Mote et al., 2005; Nazemi et al., 2013; Wheeler, 2015). Despite the need for hydrological modelling, predictive capabilities are hampered by significant limitations in our modelling ability due to, for instance, substantial heterogeneity in surface and subsurface parameters (Freeze, 1974), the fact that there is no single scale at which homogeneity of control volumes is achieved (Beven, 1989; Blöschl and Sivapalan, 1995; Klemeš, 1983; Shook and Gray, 1996), and mismatches between underlying theory and applied scales (Or et al., 2015). These limitations manifest as 1) uncertainties in model parameters, initial conditions, boundary conditions, forcing data; 2) incomplete process representations, selections, and linkages (Beven, 1993; Beven and Westerberg, 2011; Clark et al., 2008; Fatichi et al., 2016; Raleigh et al., 2015; Slater et al., 2013; Wagener and Montanari, 2011); and 3) issues of complexity including the degree of physics-based equations, the number of parameters, forcing data requirements, and spatial discretization requirements (Beven, 1993; Clark et al., 2008; Hrachowitz and Clark, 2017). Without care, physically based, mechanistic approaches can result in over parameterized models (Perrin et al., 2001) that are highly uncertain and difficult to verify (Beven, 1993). Difficulty in validating a model stems from a mismatch in model element and observed scales and limited high-resolution spatially distributed data (Beven, 1989). Physically based models should be used critically, with proper appreciation of the strengths and the limitations, and dependent on the purpose of the modelling (Beven, 1993, 2006; Das et al., 2008; Perrin et al., 2001).

Due to the significant role mountains play in global water supply as ‘water towers’ (Viviroli et al., 2007), the fragility of arctic and mountain ecosystems (Bring et al., 2016), and these regions’ sensitivity to anthropogenic climate change (Duarte et al., 2012; Mote et al., 2005; Musselman et al., 2017; Rasouli et al., 2015), there is substantial motivation to provide timely and accurate predictions in these cold regions. However, hydrological modelling in cold regions has unique challenges compared to temperate regions. Although there is uncertainty in the optimum levels of complexity required in cold region hydrological models (Avanzi et al., 2016; Clark et al., 2017), such models have unique requirements and considerations; a brief summary follows. The largest discharge event of the year often results from the melt of the seasonal snowpack (Davies et al., 1987; Gray and Male, 1981) and therefore substantial effort has been invested in snow model development, e.g., Jordan (1991), Marks et al. (1998), Bartelt and Lehning (2002), Vionnet et al. (2012), Leroux and Pomeroy (2017), and flexible snowcover modelling systems, e.g., the Factorial Snow Model (FSM) (Essery, 2015) and ES-CROC (Ensemble System Crocus) (Lafaysse et al., 2017). Streamflow discharge is impacted by snowmelt spatial heterogeneity that is due to:



variability in surface energetics (Carey and Woo, 1998; Dozier and Frew, 1990; Harder et al., 2019; Marks et al., 1992; Mott et al., 2013; Munro and Young, 1982; Olyphant, 1986; Pomeroy et al., 2003; Schögl et al., 2018), precipitation spatial variability (Harder and Pomeroy, 2013; Lehning et al., 2008; Marks et al., 2013), vegetation interception (Hedstrom and Pomeroy, 1998; Kuchment and Gelfan, 2004), and mass redistribution via wind processes (Essery et al., 1999; MacDonald et al., 2009; Mott et al., 2010; Pomeroy et al., 1993; Winstral et al., 2002). Snowmelt runoff is further complicated due to frozen soils that limit infiltration rates (McCauley et al., 2002; Zhao and Gray, 1999) such that standard infiltration representations are insufficient (Lundberg et al., 2016). Active layer depth above permafrost dramatically impacts surface characteristics (e.g., topography, vegetation, soils), streamflow seasonality, and water partitioning (Walvoord and Kurylyk, 2016). In cold regions, the numerous lakes and wetlands impact the local climate during ice-free periods (Latifovic and Pouliot, 2007; Rouse et al., 2005; Shook et al., 2015).

Numerous studies suggest that model performance is greatly improved in cold regions when including explicit spatial heterogeneity, identifiable parameter spaces, and a full range of cold regions hydrological processes, e.g., Bartelt and Lehning (2002), Bowling et al. (2004), Etchevers et al. (2004), Raderschall et al. (2008), Dornes et al. (2008b), Essery et al. (2013), Essery et al. (2009), Pomeroy et al. (2013), Fang et al. (2013), Fiddes and Gruber (2014), Kumar et al. (2013), Endrizzi et al. (2014), Mosier et al. (2016), and Painter et al. (2016). Better understanding of the physical system instead of solely focusing on parameter optimization (Bahremand, 2015) and ensuring that models are not needlessly constrained by rigidity of model structure, choice of parametrization, and representation of spatial variability and hydrological connectivity (Mendoza et al., 2015) are expected to further predictive capacity. Physics-based models may also limit the reliance upon calibrated effective values and decrease uncertainty due to requiring physically-identifiable parameters (Fatichi et al., 2016; Pomeroy et al., 2013). The use of lightly- or uncalibrated models is increasingly important for simulating future conditions as climate non-stationarity increases the uncertainty of calibrated models (Brigode et al., 2013; Vaze et al., 2010). Distributed, physics-based models are thus often the most appropriate type of hydrological model for simulating distributed state variables (Dornes et al., 2008a; Fatichi et al., 2016), simulating catchments with extreme heterogeneity (Kumar et al., 2013), or when simulating process interactions (Dornes et al., 2008a; Horne and Kavvas, 1997; Maxwell and Kollet, 2008). These improvements motivate the continued development of spatially discrete, physics-based models.

Although the need for multi-scale (Samaniego et al., 2017), hyper-resolution (sub-1 km) (Wood et al., 2011), and snow-drift resolving scales (~1 m to 100 m) (Pomeroy and Bernhardt, 2017), is becoming clear, contemporary cold-region models suffer from shortcomings when run over large extents and high spatial resolutions and may be limited to what spatial scale they operate at. In addition, these models may have limited structural flexibility for incorporating multiple modelling philosophies (e.g., Dornes et al. (2008b), Clark et al. (2011)), or have limitations in incorporating next-generation data products. In order to address the scientific and societal demands placed on hydrologic models, there is a need for a new generation of hydrological models that allow:



1. *Multi-scale, spatially distributed process representation*

Although semi-distributed schemes such as the Group Response Unit (GRU) or Hydrological Response Unit (HRU) approach have had substantial success in cold regions, e.g., Pietroniro et al. (2007), Pomeroy et al. (2007), and Clark et al. (2015), complex spatial behaviours cannot be modelled unless the HRUs are constructed *a priori* to produce the behaviours. This limits simulating cascading processes and emergent behaviours, e.g., accumulation of non-linear process interactions leading to novel, basin-wide behaviours. Representing mass and energy heterogeneities and interactions, at multiple spatial scales (Hrachowitz and Clark, 2017; Samaniego et al., 2017), and moving towards regional predictions (Sivapalan, 2017) has been suggested as a path to improving predictive capacity. Fully distributed, raster-based models are inefficient with the need for many raster cells, greatly limiting the applicability for both high resolution, and over large extents. The deficiencies in HRU, GRU, and raster-based models points towards a need for an improved terrain representation that allows both high resolution as needed and applicability for modelling over large extents.

2. *Flexible model structure*

Many models use a rigid model structure that does not allow for easily changing model algorithms nor easily testing different algorithms or hypotheses. An improved approach is to allow process modularity for easily modifying aspects of a model's structure and complexity. Such model flexibility has been present in many rainfall-runoff models, e.g., MMS (Leavesley et al., 2002), FUSE (Clark et al., 2008), SUPERFLEX (Fenicia et al., 2011), but to the authors' knowledge, such modularity in cold-region models has been limited to the Cold Regions Hydrological Model (CRHM) (Pomeroy et al., 2007) and SUMMA (Clark et al., 2015). These are both modular, physics-based, semi-distributed hydrological response unit (HRU) cold region models. A flexible model structure should allow for easily scaling between temporal scales (i.e., time-stepping), spatial extents, spatial resolutions, and process representations as required. Assumptions on explicit coupling between processes leads to difficulty in testing different process representations and limits inclusion of existing code. Despite the rich set of cold regions snow and hydrological models, e.g., Alpine3D (Lehning et al., 2006), iSnobal (Marks et al., 1998), GeoTOP (Endrizzi et al., 2014), MESH (Pietroniro et al., 2007), CRHM (Pomeroy et al., 2007), SUMMA (Clark et al., 2015), SRGM (Gelfan et al., 2004; Kuchment and Gelfan, 2004), ESCROC (Lafaysse et al., 2017), and VIC (Cherkauer et al., 2003), there are no explicitly distributed, modular cold regions models.

3. *Ease of changing model parameters, initial/boundary conditions*

Model parameters, initial conditions, and boundary conditions are uncertain in hydrological systems and are a significant constraint on model complexity and validity. Hard-coded parameters can be a significant source of uncertainty as they are effectively treated as physical constants (Mendoza et al., 2015). Modern models must be



developed so that changing initial conditions, parameters, and all aspects of the model configuration are trivial and easily done within the context of an uncertainty framework. Due to the long temporal durations for which climate change scenarios are done, flexibility in changing surface parameters with time, e.g., vegetation cover, needs to also be possible.

5 4. *Efficient use of computational resources*

10 Unlike GRU or HRU based models, distributed models are generally discretized using a raster approach with a fixed spatial resolution. This can lead to either increased computational requirements or non-optimum use of computer resources due to the over representation of the surface (e.g., homogenous locations), while choosing a coarser sized mesh may result in failure to capture quickly varying, and extremely important heterogeneity. Because of the general over representation of topography via a fixed-resolution raster, these distributed models become difficult to parametrize, and computationally expensive to run, limiting their applicability to large spatial extents. Using more efficient terrain representations as well as modern high-performance computing paradigms can reduce this wasted computational effort.

15 5. *Allow appropriate model complexity*

Raster-based models with high resolution grid cells, and wasted computational effort as noted above, often led to arbitrary complexity reduction and process removal due to computational constraints. Reducing the model runtime is often a justification for simpler conceptual models, for simpler landscape representations, and for fewer computational elements. Hydrological model complexity should be warranted based upon the simulation results and needs and not for simplicities sake.

20 Although there are substantial advantages to the benefits of using physics-based, fully distributed models, data (forcing and validation) and computational limitations that have slowed their development and adoption. However, recent technological progress has been progressively removing some of these limitations. For example, unmanned aerial vehicle (UAV) imagery is providing sub-metre digital surface and elevation maps (Bühler et al., 2016; Harder et al., 2016), vegetation classification (Spence and Mengistu, 2016), hydrological features (Spence and Mengistu, 2016), as well as initial conditions, e.g., snowcover (Bühler et al., 2016; Harder et al., 2016). Surface geophysical methods are improving characterization of large-scale subsurface properties (Hubbard et al., 2013). Remote sensing products of soil properties are of increasingly higher quality (Mohanty, 2013), and high resolution satellite imagery can be used to diagnose spatial patterns of snowcover (Wayand et al., 2018). Wide-spread access to High Performance Computing (HPC) resources, e.g., Compute Canada [Canada], Extreme Science and Engineering Discovery Environment (XSEDE) [United States], National Computational Infrastructure (NCI) [Australia], Horizon2020 initiative [European Union], can help offset the increased computational cost of the simulations and of the uncertainty analysis needed to constrain *a priori* estimated physically-based parameters



(Paniconi and Putti, 2015). Lastly, efficient uncertainty analysis frameworks such as VARS (Razavi and Gupta, 2016), can also decrease the total number of required simulations to estimate uncertainty, further reducing the computational burden. However, estimates of critical subsurface properties such as hydraulic conductivity cannot be represented a priori with sufficient confidence, nor at the correct scale, viz. effective model element parameters (Binley et al., 1989), to avoid calibration (Freeze, 1974).

In summary, models will always require a trade-off between computational complexity (e.g., algorithms, landscape representation, initial conditions, parameters, and terrain discretization) and model performance (e.g., modelled versus observed). Cold region hydrological models have unique requirements that motivate the inclusion of explicit spatial heterogeneity via semi and fully distributed discretizations. To simulate the complex inter-process interactions that lead to important hydrological features, a variety of features must exist within a distributed, process-based modelling framework.

This manuscript outlines the philosophy and details of a new hydrological model, the Canadian Hydrological Model (CHM), and how the development of this modelling framework addresses the above outlined limitations of many existing hydrological models and contributes to cold regions modelling. This manuscript focuses on the overall model philosophy and design, and provides a small number of cold-region specific features and examples.

4 — Design and Overview

4.1 — Overview

The Canadian Hydrological Model (CHM) is a spatially distributed, modular modelling framework. Although not restricted to cold regions, it is designed with cold region processes in mind and has various capabilities that facilitate the modelling of these domains. The design goal of CHM is to use existing high quality open source libraries and modern high-performance computing (HPC) paradigms. By providing a framework that allows for as loose or tight a coupling between processes as required, CHM allows integration of current state-of-the-art process representations and makes no assumptions about the complexity of these process representations. It allows testing of the representations in a consistent manner, diagnosing model behaviour due to parameter changes, process representation changes, basin discretization, etcetera. Spatially, it allows for domains at point (10^{-6} km²), hillslope (1 km² to 10 km²), basin (100 km²), regional (8000 km²), and provincial/state (> 1 000 000 km²) scales. The following sections outline the framework features, including terrain representation, surface parameterization, process representation, meteorological inputs, parallelism, uncertainty analysis, visualization and analysis, and adaptation of raster algorithms. Additional model components are being developed, and will be available in future versions of CHM.



4.2 — Terrain representation

The spatial variability of terrain is a key component to any model and is an important component of model complexity. Regardless of how sophisticated, physics-based, and spatially explicit a hydrological model may be, at some level the hydrological system is conceptualized and aggregated into a control volume (Vrugt et al., 2008). Structured meshes, also known as rasters and grids, are a landscape discretization where the landscape is discretized by uniform sized cells. Raster-based hydrological models are common (Tucker, 2001) because their computer representation is trivial, and widespread use of rasters, such as in remote-sensed data, makes using them a natural choice in hydrological models. However, rasters have a number of significant limitations, the most limiting being a fixed spatial resolution over the entire basin (Tucker, 2001). This results in potentially large computational inefficiencies due to over-representation of topography. This arises as a result of requiring small raster cells (elements) to capture the spatial variability in areas of high topographic variability or (sub-) surface variability (e.g., vegetation, soils), which results in over-representation of areas that have limited spatial variability. Coarse resolution rasters also have discontinuities in the elevation data, where adjacent cells may have large elevation differences.

Unstructured triangular meshes, sometimes referred to as Triangulated Irregular Networks (TINs), represent the topography via a set of irregularly sized, non-overlapping connected triangles, where each triangle face is of a constant gradient (Chang, 2008). Areas of large topographic variability can have a higher density of small triangles in order to capture the spatial variability and areas of relatively homogeneous topography have fewer large triangles. This a more efficient terrain representation than rasters (Shewchuk, 1996), and may have up to a 90% reduction in computation elements (Ivanov et al., 2004; Marsh et al., 2018). Despite these computational advantages, a practical downside is that due to the widespread availability of raster data, conversion to an unstructured mesh is required. This results in increased uncertainty due to aggregation of the landscape into control volumes. The CHM uses a novel multi-objective approach for unstructured triangular mesh generation, *Mesher*, detailed in in Marsh et al. (2018). A brief summary follows: quality Delaunay meshes are generated ensuring a smooth graduation between small and large triangles; triangles are bounded with minimum and maximum triangle areas to ensure process representations match the physical scale; triangles are generated to fulfil tolerances (e.g., RMSE) to the underlying topographic raster and other important landscape features such as vegetation and soils. This mesh generation attempts to limit the amount of error introduced by the approximating surface given by the unstructured mesh and provide mechanisms to ensure spatial heterogeneity in the landscape is correctly preserved.

Using this mesh generation, simulation domains can be constructed at a variety of spatial extents, and importantly, spatial scales. An example of this variable resolution triangulation mesh for a region west of Calgary, Alberta, Canada in the Canadian Rockies is shown in Figure 1. The triangular edges are shown in grey lines. The variable resolution produces larger triangles in the valley bottoms, where topographic variability is limited, and small triangles in the mountains, where the



heterogeneity is greater. This allows for diagnosing the impact of scale on model performance as well as matching the process representation to the correct model length scale. Further constraints could ensure streams are accurately defined.

4.3 — Triangle parameterization

Setting values of parameters for the triangles, such as assigning vegetation or soil to the triangle, is done during the mesh generation phase. The parameter values are stored in a file separate from the underlying mesh, and thus can be easily changed at run time. This allows for easily investigating the impact of parameter values on outputs. The parameterization of the triangles is done by a) determining the valid raster cells under each the triangle and b) calculating an area-average metric for these cells and assigning this value to the triangle. Maximum and mean are the two most commonly used methods, but it can be any user-defined function. For classified data, the mode is used. This would allow, for example, selection of the most dominant landcover class. In addition, a user-specified classifier function can be given to easily classified continuous input parameters; e.g., classifying vegetation-heights into vegetation classes. Lastly, CHM provides mechanisms to write model output to a format that can be used as input; that is, CHM can use its output to set triangle values for future simulations.

4.4 — Modular process representation structure

A hydrological model is a hypothesis based on assumptions of how a hydrological system works (Savenije, 2009). Modular model structures allow for rigorously testing process representations and have been used with success in cold regions hydrology, e.g., Cold Regions Hydrological Model (CRHM) (Pomeroy et al., 2007), and Structure for Unifying Multiple Modeling Alternatives (SUMMA) (Clark et al., 2015). A key feature of CHM is that it provides a modular process representation that is suitable for distributed modelling, while maintaining high computational performance and flexibility.

In CHM, process representations are conceptualized into *modules*. A principal design goal of the module system is that a module has an enforced set of pre- and post-conditions. Pre-conditions represent the variables that must be computed prior to a given module running, and post-conditions encapsulate variables that must be computed by the currently running module so-as to be available as input for other modules. At run time, the user-selected set of modules are linked together into a directed acyclic graph based on these variable dependencies, and module execution order is determined via a topological sort of this graph. This sort ensures that modules are run in an order so-as to fulfill the pre-condition (i.e., the variable dependencies). Linkages between modules showing these dependencies are shown in Figure 2. The lines with arrows show how variable dependencies are resolved between modules. The lines going from a module are the post-conditions that satisfy the pre-conditions of the next-to-be-run module. In this example, a snowcover model, Snobal, is being driven by meteorology with the output of Snobal being used as input to a frozen soil infiltration model (Gray_inf).

The hydrological literature has a diverse set of process representations that are either one-dimensional with no lateral exchange between elements (point-scale) or are explicitly coupled with surrounding elements (Todini, 1988). CHM makes



no assumption about either, and modules may either operate on a single triangle, or on the entire domain. If only point-scale modules are selected, then CHM may be optionally run at a point-scale, effectively disabling the rest of the distributed framework. As there are substantial merits to mixing top-down and bottom-up process representations (Hrachowitz and Clark, 2017), CHM makes no assumptions on the complexity or type of process representation a module – modules may be a mix of complex physics based representations and conceptual representations. This also applies to process coupling. For example, a module could be a single process (e.g., a snow model), a coupled set of processes (e.g., coupled heat and energy snowmodel + frozen soil routine), or an entire existing model.

Due to the strict pre- and post-conditions required for module dependency resolution and the abstraction used in CHM, existing libraries and code can be used in a model. There is no need to rewrite the code. Therefore, any code that may be called via a C interface (e.g., Fortran, R, Python, Matlab) is suitable to be used (with a few considerations) as a CHM module. Shown in Table 1 are a list of the processes currently available in CHM.

4.5 — Input meteorology

Input meteorology is prescribed as a point source (herein, ‘virtual station’) defined by latitude, longitude, and elevation. However, a virtual station may have an arbitrary location and elevation and need not be within the simulation domain, nor correspond to a real meteorological station. This allows a virtual station to be located at, for example, the centre of a numerical weather prediction output grid centre. Because all input meteorology is given as a point source, various spatial interpolates are present in CHM to provide a distributed field across all triangles.

Spatial interpolates are present as inverse distance weighting (IDW) and thin plate spline with tension. In some cases, no interpolation is desired, and therefore a third option called ‘nearest’ is available – this uses the nearest virtual station without any spatial interpolation. Over large domains, such as when using numerical weather prediction output, every virtual station in the simulation domain should not be used in the interpolation to every triangle. Therefore, interpolates may query a list of either: a) virtual stations within some distance of the triangle or b) the closest n virtual stations. This ensures that only nearby virtual stations are used to form the interpolant. Vertical elevation correction for elevation is provided by a set of specialty modules. All virtual stations are corrected to a common reference level using these modules prior to spatial interpolation. A list of these algorithms is given in Table 2.

Input meteorology may be given as either text files or as NetCDF files (Rew and Davis, 1990). When NetCDF files are used, the timesteps’ data are lazy-loaded such that only the current timestep is read. This decreases the up-front load time as well as decreases total memory usage. An example of NetCDF usage is shown in Figure 3 for a domain west of Calgary, Alberta, Canada over the Bow River Valley (red = high elevation, blue = low). Virtual stations are shown in black and these correspond to the cell centres from the 2.5 km Global Environmental Multiscale (GEM) model (Côté et al., 1998) 2-day forecast.



4.6 — Input filters

Input filters provide a mechanism to modify input meteorology during runtime. This is similar to the filter feature in MeteoIO (Bavay and Egger, 2014). Filters are assigned to each virtual station, and each virtual station may have an arbitrary number of filters. The purpose of filters is to allow, for example, values outside of a certain range to be filtered, or to perform a correction such as taking an observed windspeed at 2 m and changing it to 10 m for use later in a process module. Filters operate per-timestep and therefore can consider the previous model timestep for use in the correction; e.g., including snowdepth to perform vertical windspeed height correction.

4.7 — Point mode

Due to the difficulty in validating spatial models due to limited spatial observations, evaluation is generally performed using point observations. CHM may be run in point-mode that allows for simulating a single triangle using a specialized input module to pass a hydrometeorological station's observation data directly to the underlying process models. This is intended to simulate a point collocated with an input observation meteorology dataset and allows for traditional point simulations.

4.8 — High Performance Computing

In CHM, parallelism is currently implemented via the shared memory OpenMP library. Coding a process representation into a module will generally result in either a point-scale module (e.g., point-scale snowcover model) or it will be a spatially coupled model (coupled advection-diffusion equation). The first type, owing to the fact it does not require knowledge of its neighbours to compute a value, corresponds to an embarrassingly parallel problem. Herein, these are referred to as data parallel. Spatially coupled models require the solution at their neighbour triangles in order to compute a solution. These neighbours, in turn, require solutions at *their* neighbours, and so on. Therefore, this is a much more challenging type of problem to introduce parallelism to. Herein, these are referred to as domain parallel. Data parallel modules automatically have the parallelism implemented and require no special consideration from the developer. Domain parallel modules, however, require the module developer to implement parallelism as appropriate for the module.

Mixing these two types of parallelism complicates the implementation of parallel code. To provide as much seamless parallelism as possible, each module declares the type of algorithm it is: data parallel or domain parallel. After the topological sort is performed to determine module execution order, the modules are scheduled together into groups that share a parallelism type. For example, consider the following sorted list of modules, with their parallelism type in brackets:

mod_A (parallel::data)

mod_B (parallel::data)

mod_C (parallel::data)



mod_D (parallel::domain)

mod_E (parallel::data)

These would then be scheduled together into 3 groups:

Group 1

5 mod_A (parallel::data)

mod_B (parallel::data)

mod_C (parallel::data)

Group 2

mod_D (parallel::domain)

10 **Group 3**

mod_E (parallel::data)

The modules in group 1 are run in parallel together. Because they are data parallel, only one iteration over the mesh is required. Then, groups 2 and 3 are run. This scheduling mechanism reduces the overhead of a modular approach by limiting total iterations over the mesh and minimizing thread creation. Further, as most hydrological process representations are point-scale, it allows for abstracting parallelism, resulting in “free” parallelism for the developer.

4.9 — Uncertainty analysis

CHM provides a mechanism to easily allow modules to obtain parameter values from configuration files (JSON format), overriding the default hard-coded value. Changes to the model structure (i.e., choosing modules), initial conditions, and parameter files (e.g., landcover) are also done via this mechanism. Users may, via the command line, change any configuration value – thus simplifying uncertainty testing. This mechanism reduces situations where changes require re-compilation.

The Python code snippet shown in Listing 1 demonstrates changing values on the command line (via Python). This code is setting the name of three output files and adding a new module to be run.

Listing 1: Example to setting output file names and adding a new module.

```
25 import subprocess  
import shutil
```



```
prj_path = "CHM.config"
```

```
cf1 = "-c output.VistaView.file:vv_dodson.txt"
```

```
cf2 = "-c output.UpperClearing.file:uc_dodson.txt"
```

```
5 cf3 = "-c output.FiserraRidge.file:fr_dodson.txt"
```

```
cf4 = "--add-module Dodson_NSA_ta"
```

```
subprocess.check_call(['./CHM %s %s %s %s %s' % (prj_path, cf1, cf2, cf3, cf4)], shell=True)
```

4.10 — Visualization and analysis

10 The output format used is the ParaView (Ahrens et al., 2005) unstructured mesh format. This allows for visualization of the simulation results in full 3D, with timeseries analysis in ParaView, as shown in Figure 4. The addition of a ParavView plugin for CHM allows for displaying the date and time of the output. The animation view allows for exploring the spatio-temporal results in the results. It also allows for immediate diagnosis of modelling errors. There are many post-processing filters and tools available in ParaView, such as plotting an individual triangle's values over time. Because ParaView uses the
15 Visualization Toolkit (VTK) library (Schroeder et al., 2006), the ParaView files can easily be loaded and post-processed using the Python VTK library in conjunction with traditional Python libraries such as NumPy (E, 2006) and SciPy (Jones et al., 2018).

In addition to the ParaView output, CHM provides a set of post-processing scripts that allows for converting the Paraview file to a rasterized GeoTiff or NetCDF file. This allows for using the output in post-processing algorithms that require arrays,
20 or in GIS.

4.11 — Adaptation of raster-based algorithms

Adaptation of raster-based algorithms is an important aspect of CHM as many existing algorithms are raster-based. Frequently, raster-based algorithms employ logic that performs queries such “look X length units in direction Y”. This is easily done on a structured mesh, however on an unstructured grid, this process is non-obvious. Iterating over each triangles’
25 neighbours results in a random walk across the domain, and brute-force iteration search methods are needlessly slow. CHM uses the *k*-d spatial search tree available within the dD Spatial Searching (Tangelder and Fabri, 2018) package in the Computational Geometry Algorithms Library (CGAL) to optimize spatial queries. Briefly, a *k*-d tree is a generalization of a binary search tree in high dimensions that decomposes the search domain into a set of small sub-domains (Bentley, 1975). This tree structure can then be reclusively searched resulting for efficient spatial look-ups. The *k*-d tree implementation is
30 how nearby stations are determined. This technique for spatial searching can also be used to calculate terrain parameters, such as the terrain curvature.



5 — Model application

5.1 — Overview

The following section describes the methodology for evaluating various features of CHM as well as providing examples of usage. Although the CHM will eventually include the entirety of the hydrological cycle, snow accumulation and surface meteorology processes are currently implemented. Marmot Creek Research Basin (MCRB) in the Canadian Rockies in Alberta, Canada is used as a location to test the two snow models and various models to provide the driving meteorological forcing for these models that are currently implemented in CHM. The meteorological interpolants are tested in a leave-one-out validation across the MCRB. In addition, an adaptation of a raster-based terrain-shadowing for shortwave irradiance calculation is presented, demonstrating the conversion of an algorithm from a raster to unstructured mesh. Finally, the parallel computation aspect of CHM is tested by performing a scaling analysis using different number of CPUs.

5.2 — Study Site

5.2.1 — Marmot Creek

Marmot Creek Research Basin (MCRB) (Golding, 1970) is located in the Kananaskis River Valley of the Canadian Rockies, as shown in Figure 5. It is a 9.4 km² basin covered predominately by needle-leaf forest (Fang et al., 2013). The climate is dominated by continental air masses with long and cold winters; however these are interrupted by frequent chinooks (Foehns) in mid-winter (DeBeer and Pomeroy, 2009). It spans an elevation range from 1700 m to 2886 m (Rothwell et al., 2016) and snow covers the upper elevations of the basin from October to June. The average seasonal precipitation is approximately 600 mm at low elevations increasing to over 1140 mm at the tree line (Rothwell et al., 2016).

5.2.2 — Meteorological observations

Meteorological observations for air temperature, relative humidity, wind speed, precipitation, soil temperature, and incoming shortwave radiation for the Upper Clearing site (1860 m), Vista View (1956 m), and Fisera Ridge (2325 m) sites, shown as crosses in Figure 5, were used. Gap filled, quality corrected 15 min data for the water years 2007 to 2016 (inclusive) were used. Please see Fang et al. (2019) for further details. Precipitation was measured with Alter-shielded Geonor weighing precipitation gauges and corrected for wind-induced under-catch (Smith, 2009). Precipitation phase was determined via the psychrometric energy balance method of Harder and Pomeroy (2013). Longwave irradiance was calculated following Sicart et al. (2006). This was developed for mountainous terrain and was shown to have an error of less than 10% over the snowmelt season. This method has been used with success at the MCRB.

Periodic snow surveys of depth and SWE on long transects at Upper Clearing were conducted by various members of the Centre for Hydrology and used to quantify snowpack density. For each transect, there were at least 25 snow depth measurements and at least 6 gravimetric snow density measurements using an ESC-30 snow tube (Fang et al., 2019).



5.3 — Models

5.3.1 — Snowmodels

Point-scale evaluation of the two snowmodels in CHM, Snobal and Snowpack, was done at the Upper Clearing site.

5 Snobal (Marks et al., 1999) is a physics-based, two layer snowpack model designed specifically for deep mountain
snowpacks and approximates the snowpack by two-layers where the surface fixed-thickness active layer (taken here as 0.1
m) is used to estimate surface temperature for outgoing longwave radiation and atmosphere-snow exchange of sensible and
latent heat via turbulent transfer. Snobal features a coupled energy and mass balance, internal energy, and liquid water
storage calculations. Turbulent fluxes are explicitly calculated via Marks et al. (1992), a bulk transfer approach that includes
a Monin-Obukhov stability correction. The ground heat flux is calculated from conduction with a single soil layer of known
10 temperature.

Snowpack (Bartelt and Lehning, 2002; Lehning et al., 2002) is a multi-layer finite element model of mountain snowpacks,
with application for avalanche hazard forecasting. It describes the microphysical properties of a snowpack and includes the
dynamic addition/removal of snow layers using a system of PDEs. These are discretized vertically into an arbitrary number
of snow layers in a Lagrangian coordinate system. It has a coupled energy and mass balance, internal energy, and liquid
15 water storage calculations with a bulk-transfer turbulent flux scheme with Monin-Obukhov stability correction (Michlmayr
et al., 2008).

Both Snowpack and Snobal were configured to use the albedo routine of Verseghy et al. (1993). The snow models are driven
with observed precipitation, shortwave irradiance, wind speed, air temperature, relative humidity, and soil temperature at a
15-minute time interval. Because of the sheltered nature of the the Upper Clearing, no blowing snow was simulated
20 (Musselman et al., 2015). Snowmodel parameters, such as roughness length, were set following Pomeroy et al. (2012).

5.3.2 — Mesh generation

The unstructured mesh was created using the *Meshier* software. A 1 m x 1 m input elevation LiDAR DEM (Hopkinson et al.,
2011) was used. The resulting mesh was generated to have a minimum triangle area equivalent to a 25 m x 25 m raster and
represented the topography to within 25 m RMSE. This resulted in approximately 45,000 triangles.

25 5.3.3 — Raster algorithm adaptation (shadowing)

An example of the adaptation of a raster algorithm to the unstructured mesh is shown for a terrain shadowing algorithm that
calculates the shadows cast from surrounding terrain. The “look X length units in Y direction” query is required for finding
obstructing terrain (e.g., a tall mountain) by searching along the azimuthal direction towards the sun. As a demonstration of
the *k-d* tree usage in CHM, the shadowing algorithm of Dozier and Frew (1990) (herein DF90) was implemented for



unstructured triangular meshes. In brief, the DF90 algorithm searches along an azimuthal direction within some horizontal distance and attempts to find terrain that is above the solar elevation. This is illustrated in Figure 6. For an observer A , a search along the azimuth that corresponds to the solar vector S is performed. For each terrain element found, a new vector (H) is calculated. If the slope of H is greater than that of S , A is in shadow. Terrain is searched from the observer towards
5 some maximum search radius, in steps of size dx . Specifically, this adaptation of DF90 required using the k -d tree to find the triangle at a distance X m from the source triangle (A) along an azimuth that corresponded to the solar vector, S .

The DF90 shadowing algorithm was run for all of Marmot Creek, using the mesh described in Section 3.2. A maximum search radius of 1000 m was used, discretized into 10 steps. The DF90 implementation was compared to: observed shadowed area (see below), the Marsh et al. (2012) shadowing model, and the Solar Analyst (Fu and Rich, 1999) shadow model. Solar
10 Analyst is an extension in the ArcGIS software by Environmental Systems Research Institute (ESRI). The observed shadowed area are from time-series images from the field campaign detailed in Marsh et al. (2012) and were orthorectified using the software of Corripio (2004). Shadow location for February 1, 2011 at 17h00 was used in this comparison. The output from CHM was rasterized from the unstructured mesh at a 1 m x 1 m spatial resolution.

5.4 — Leave one out comparison

15 To test the efficacy of the meteorological interpolates, a leave-one-out comparison was conducted for the Upper Clearing, Vista View, and Fisera Ridge stations. This entailed using two of the three meteorological stations as input for CHM, in order to predict the third. For example: Upper Clearing and Vista View were used to predict meteorological conditions at Fisera Ridge; Vista View and Fisera Ridge were used to predict Upper Clearing; et cetera.

A ten-year period using 15-minute data were simulated. The following meteorological interpolants were used: terrain shadowing (Dozier and Frew, 1990), cloud fraction (Walcek, 1994), air temperature (Cullen and Marshall, 2011), relative
20 humidity (Kunkel, 1989), precipitation phase (Harder and Pomeroy, 2013), precipitation (Thornton et al., 1997), and solar radiation transmittance estimated from observed incoming shortwave values.

5.5 — Parallel scaling

The heterogeneous Westgrid cluster Graham was used to investigate the scaling performance of the CHM code with various
25 numbers of CPUs. The base nodes were used. These have two Intel E5-2683 v4 Broadwell CPUs at 2.1 Ghz for a total of 32 cores and 128GB of RAM. The modules run include the data parallel Snobal snowpack module, as well as a domain parallel advection-diffusion blowing snow module (Marsh et al., 2019 in review).

Simulations were run for a mesh with $\approx 100,000$ triangles. The model was run with 1, 2, 4, 6, 8, 16, and 32 cores, and for each core-count scenario, the fastest of 5 runs was taken. File output was disabled for these runs. The speedup for the n core
30 run ($core_n$) was computed relative to the 1-core run ($core_1$):



$$\text{speedup} = \frac{\text{core}_1}{\text{core}_n}. \quad (1)$$

6 — Results

6.1 — Point scale snowmodel

Shown in Figure 7 is the simulated snow water equivalent (SWE [mm]) for Snowpack (blue) and Snobal (red). The water
5 year is denoted above each plot. Snow course observations are shown as black dots. The RMSE and MB values for both
models, for each water year, are shown in Table 3.

In 2007, Snowpack over estimates peak SWE more than Snobal, although ablation timing between the two is identical. In
2007, early season SWE is over estimated by Snowpack although late season SWE is better estimated by Snowpack. Water
year 2009 is poorly simulated in general, especially by Snobal. It is not clear what causes this poor performance. During the
10 cold winters of 2010 and 2011, both models perform well. In 2012, Snobal underestimates peak SWE versus Snowpack. For
years 2013 to 2015 Snowpack better captures peak snow and the ablation period than Snobal. In 2016 Snobal better
estimates SWE as Snowpack overestimates during accumulation and for peak SWE. Snowpack tends to be more consistent
in its prediction capacity, although it tends to over estimate, whereas Snobal tends to underestimate total SWE. Overall
Snowpack tends to perform better than Snobal, although there are individual years where Snobal edges out Snowpack.

15 6.2 — Adaptation of raster-based algorithm

Shortwave irradiance corrected for slope and aspect, with horizon (cast) shadows via an adaptation of the Dozier and Frew
(1990) shadowing algorithm for unstructured meshes for the Marmot Creek Research Basin is shown in Figure 8. Simulation
is for 2011-02-01 17:00 local time. High irradiance is shown in red, and shadows shown in dark blue; and these areas are
receiving only diffuse radiation. The region shown in the red square is shown in detail in Figure 9. This figure shows an
20 orthorectified terrestrial photo of a shadow passing over Mt. Collembola from Fisera Ridge. The location of the shadowed
region for 2011-02-01 17:00 local time is shown for the DF90 algorithm described herein (green), the observed shadow
(red), the ArcGIS Solar Analyst shadow (black), and for the Marsh 2012 algorithm (blue). The DF90 implementation agrees
quite well with observed shadow locations and a sensitivity test (not shown) shows improved agreement with increasingly
small triangles. The triangular shaped bumps along the shadow line are from the unstructured triangular mesh elements.

25 6.3 — Leave one out validation

The leave one out validation is shown in Figure 10 for Vista View (top row), Upper Clearing (middle row), and Fisera Ridge
(bottom row). The dashed line is the 1:1 line, and the solid black line is a linear regression line of best fit. The r^2 value for
this fit is shown in the bottom right corner. Due to significant over-plotting of the data points, the values have been binned



into 100 hex-bins and coloured using the log of the normalized per-bin count. Grey values are bins that have a normalized count of less than 0.01. Because of the significant number of low and zero values in the shortwave and precipitation timeseries, this resulted in the per-bin colouring being difficult to read. Values of ISWR $< 50 \text{ W m}^{-2}$ and $p < 1 \text{ mm}$ were removed for the colouring. Please note that these data *were not removed* for the linear fit, r^2 , MBE, or RMSE metrics.

5 Temperature was well predicted at all sites with r^2 values of 0.99, 0.97, and 0.92 for Vista View, Upper Clearing, and Fisera Ridge respectively. Both mid-elevation sites were better predicted than the high elevation (Fisera Ridge) site. The majority of the data lies close to the 1:1 line. Upper Clearing had a warm bias (MB=1.11 °C), whereas Fisera Ridge had a cold bias (MB=-0.37 °C). Less spread was observed in the summer months (not shown), matching the results of Cullen and Marshall (2011). Relative humidity was the most poorly predicted variable. Vista View was the most accurately predicted ($r^2=0.9$)
10 with a slight (1.09%) positive bias. Upper Clearing had more spread with a distinct negative bias (-6.2%) and decreased r^2 (0.76). Fisera Ridge was exceptionally poorly predicted ($r^2=0.55$, MB=6.12%). A separate analysis that grouped the data into winter and summer periods (not shown) showed improved results and less spread during the summer months, especially for Fisera Ridge; this summer period had: $r^2=0.7$, MB=7.84%, RMSE=15.32%. Due to the proximity to vegetation, summer evapotranspiration may result in less temporal variability, dampening the responses. The interpolation methods assume a
15 free-atmosphere, and thus do not capture these canopy impacts. During the winter months, the observed RH is predominately dominated by synoptic scale forcing (Cullen and Marshall, 2011) and may be influenced by the sublimation of intercepted snow in the canopy (Pomeroy et al., 2012) which are not captured by this interpolation. The Fisera Ridge data has had substantial infilling for the RH variable (Fang et al., 2019), and the poor fit of CHM to these infilled data may be as a result of the infilled data using a higher elevation, exposed ridge, that may not be representative of Fisera Ridge. Shortwave
20 irradiance is generally well captured, although Fisera Ridge has a larger negative bias (-15.79 W m^{-2}) than the other two sites. Precipitation at Vista View and Upper Clearing was well predicted, and Fisera Ridge is again the least well predicted.

6.4 — Parallel scaling

Shown in Figure 11 are the scaling results for 1, 2, 4, 6, 8, 16, and 32 cores. Good scaling is observed with a 1.97x speedup with 2 cores, 7.23x speedup with 8 cores, a 12.3x speedup with 16 cores, and a 20.5x speedup with 32 cores. A sub-linear
25 scaling is expected due to the mixing of domain and data parallel modules. As most compute nodes are approximately 32 cores, this shows good per-node scaling and thus demonstrates motivation for moving towards a distributed memory model, such as MPI.

7 — Conclusion

Simulations of hydrological phenomena are increasingly important for management and prediction of the hydrological cycle
30 under anthropogenic climate change impacts. Cold regions are some of the most sensitive regions to these impacts. However,



they have unique modelling challenges. Increasing importance is being given to rigorous uncertainty analysis, process representation testing, and multiple hypothesis testing. Spatially distributed models are generally thought to produce improved predictions in cold regions when spatially explicit prognostic variables are required, however substantial challenges including initial conditions, boundary conditions, parameterizations, and computational costs all conspire to limit their applicability. Despite this, hyper-resolution models are increasingly being applied for water management and design decisions.

There is a significant opportunity for next-generation models to address challenges in existing models and adapt the large successes from hydrological modelling. These challenges include seamless prediction at various spatial and temporal scales, utilization of hyper-resolution data obtained by new remote sensing platforms, quantify of structural uncertainty in distributed models, and utilization of modern high-performance computing infrastructure.

In this paper, a new modelling framework, the Canadian Hydrological Model (CHM), was presented as a first step towards these goals in cold regions. A new unstructured mesh implementation of the well-known Dozier and Frew (1990) shadowing algorithm was derived to demonstrate adaptation of raster-based algorithms. Key features of CHM include the ability to capture spatial heterogeneity in an efficient manner; to include multiple process representations; to be able to change, remove, and decouple hydrological process algorithms; to work both at a point and spatially distributed; the ability to scale to multiple spatial extents and scale; and to utilize a variety of forcing fields (boundary and initial conditions).

8 — Author contributions

C. Marsh: Initial idea, coding, analysis, manuscript preparation

J. Pomeroy: Idea refinement, analysis refinement, manuscript revision

20 H. Wheeler: Idea refinement, manuscript revision

9 — Acknowledgments

The authors would like to acknowledge the financial support of the Canada Excellence and Canada Research Chairs programmes, the Natural Sciences and Engineering Research Council of Canada's Discovery Grants, Alexander Graham Bell Scholarships and Changing Cold Regions Network, Alberta Innovates, and the Canada First Research Excellence Fund supported Global Water Futures programme. Marmot Creek logistical support from the Nakiska Ski Resort and fieldwork support from Michael Solohub, May Guan, Angus Duncan, Greg Galloway and many others are gratefully noted.



10 — Code availability

The code for the Canadian Hydrological Model is open-source under the GPLv3 license and is available at <https://github.com/Chrismarsh/CHM>. The mesh generation software, Mesher, is open-source under the GPLv3 license. It is available at <https://github.com/Chrismarsh/mesher>

5 11 — Figures

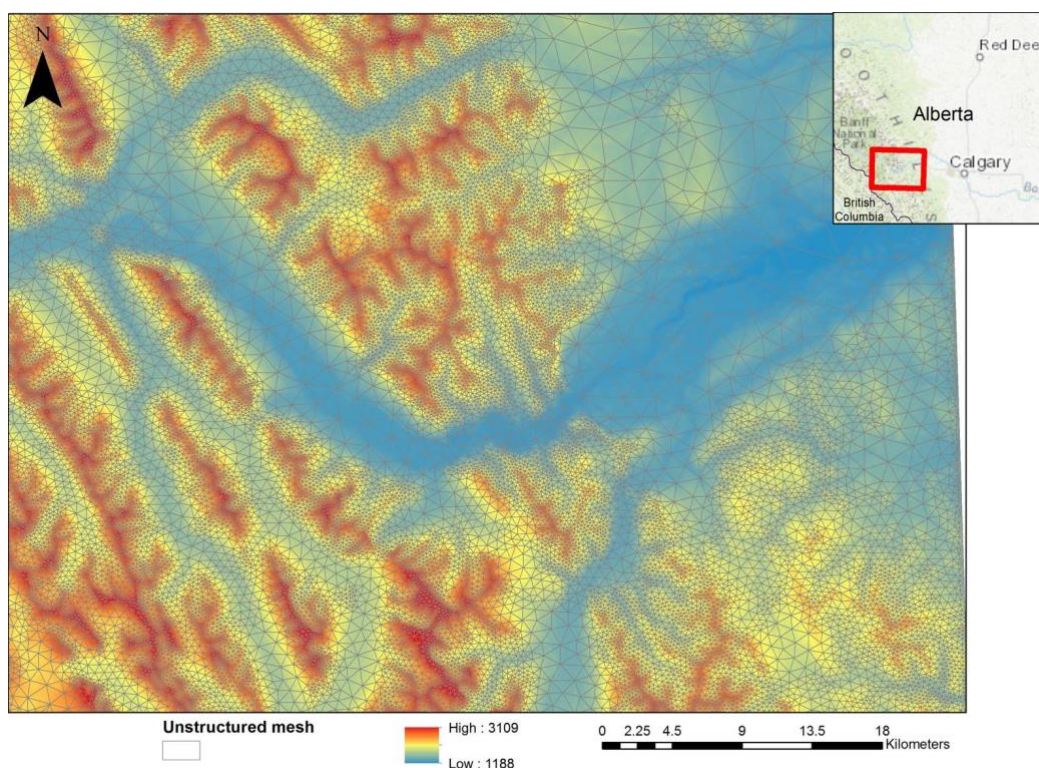


Figure 1: Example of variable resolution triangulation mesh as produced by Mesher for a region west of Calgary in the Canadian Rocky Mountains. The triangular edges are shown as grey lines overlain on the original DEM.

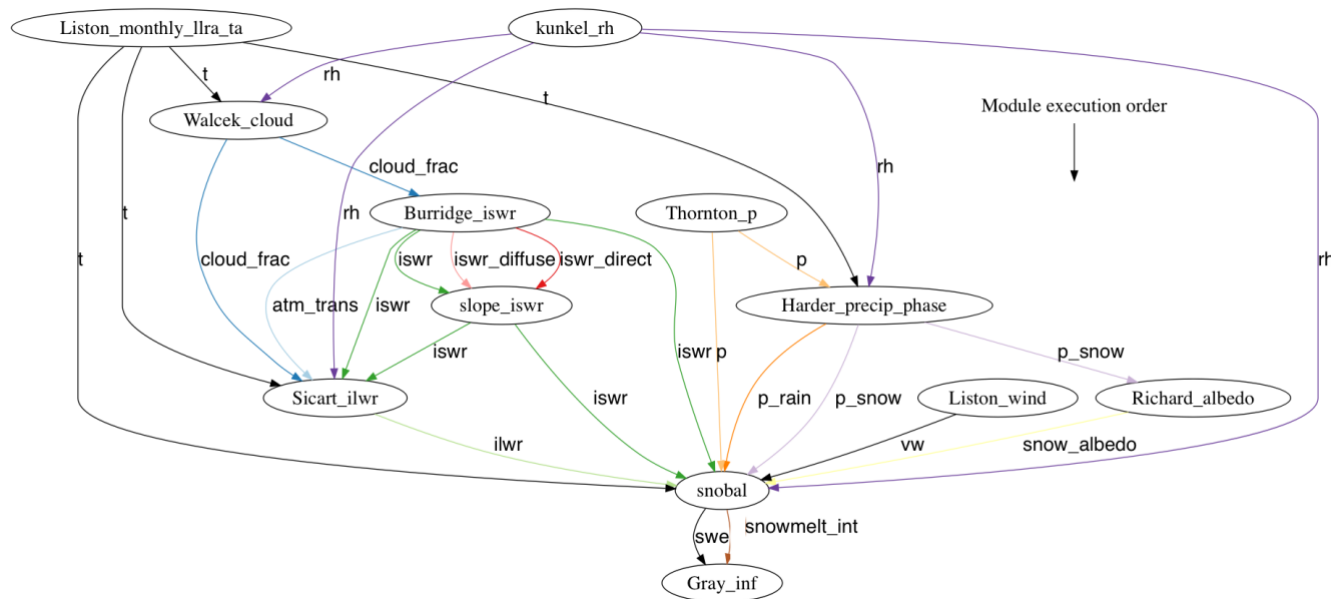


Figure 2: Directed acyclic graph showing module dependencies. Lines point to the module that requires the listed dependency. In this example, a snowcover model, Snobal, is being driven by meteorology in order to drive a frozen soil infiltration model (Gray_inf)

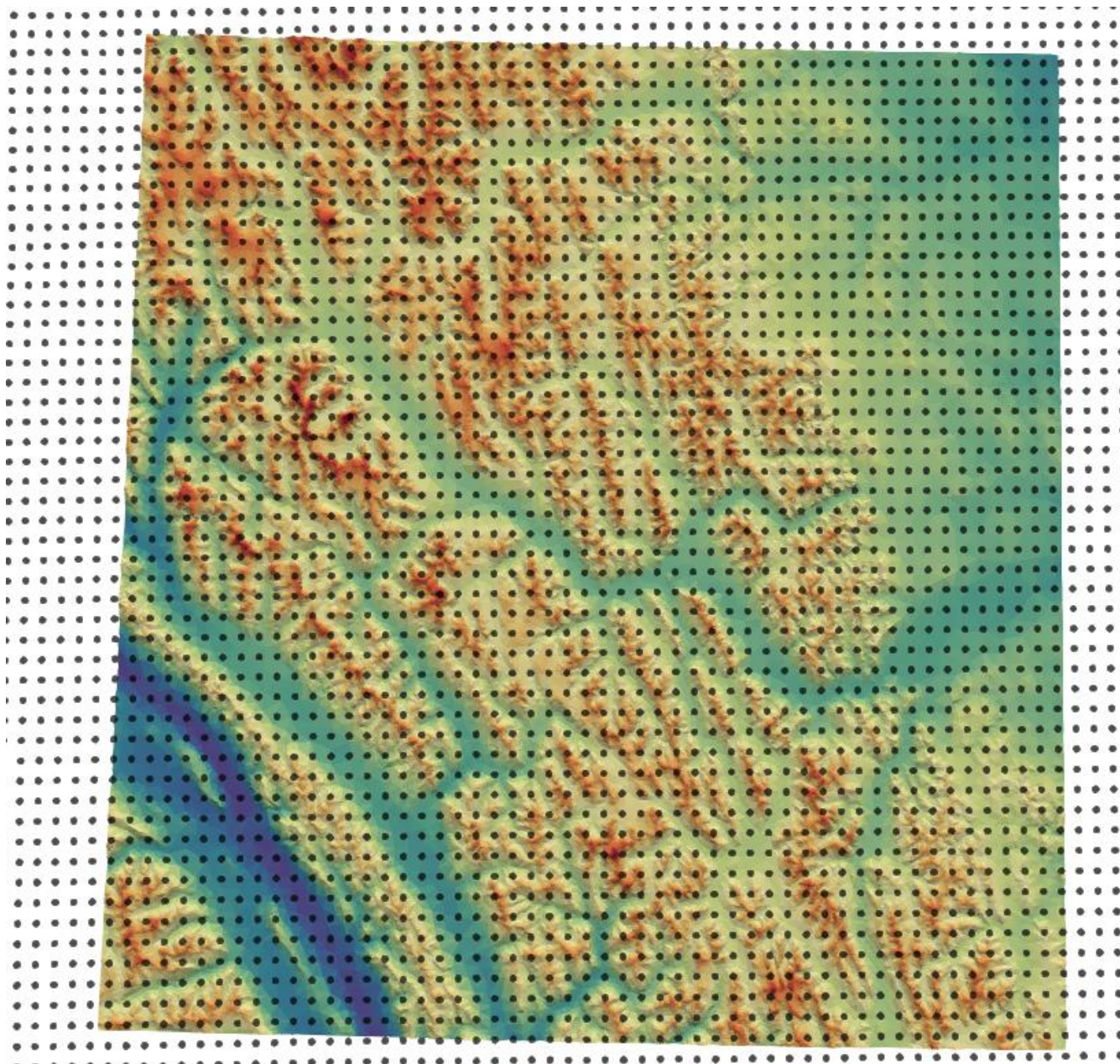


Figure 3: A domain west of Calgary, Alberta, Canada over the Bow River Valley is shown (red = high elevation, blue = low), with virtual stations, shown in black, that correspond to the cell centres from the 2.5 km GEM 2-day forecast.

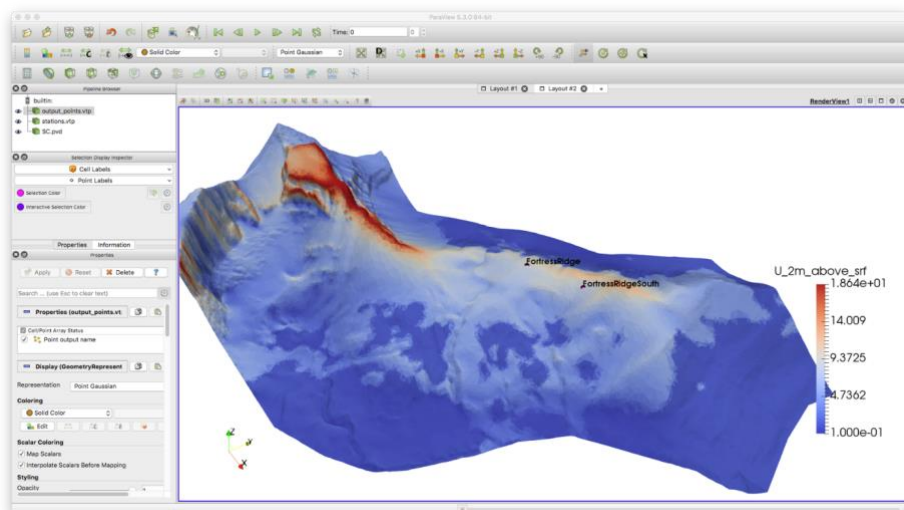


Figure 4: Output from CHM is in the ParaView format, allowing for timeseries analysis and full 3D visualization in ParaView.

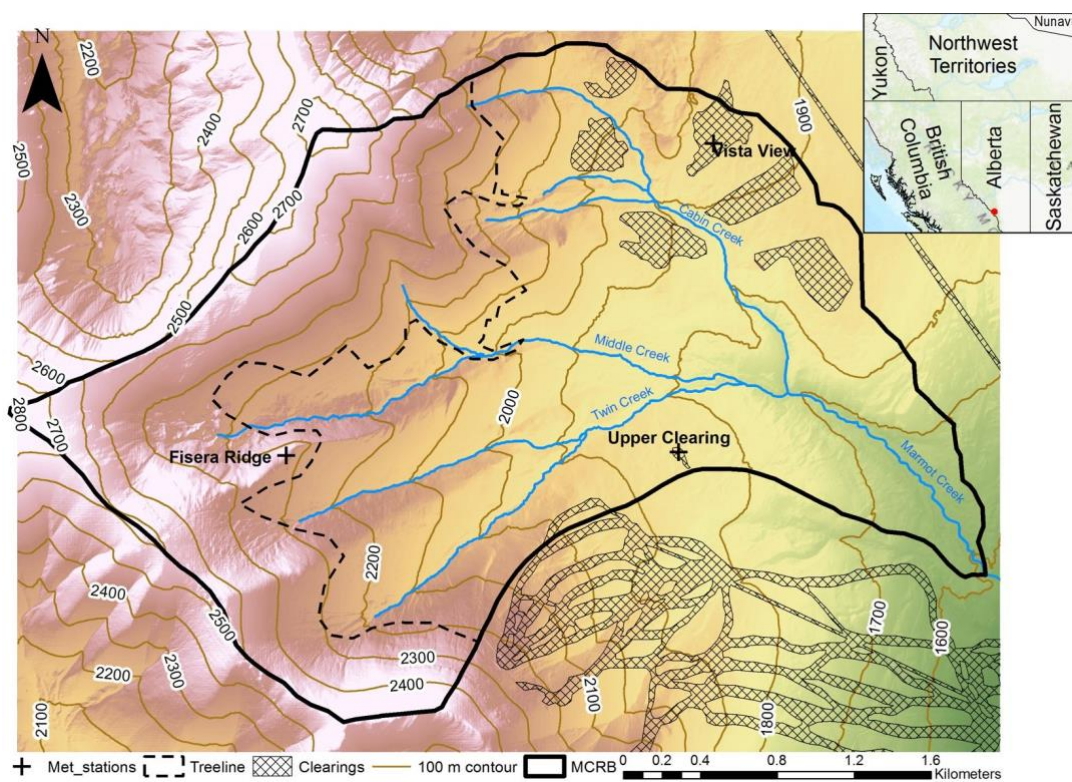
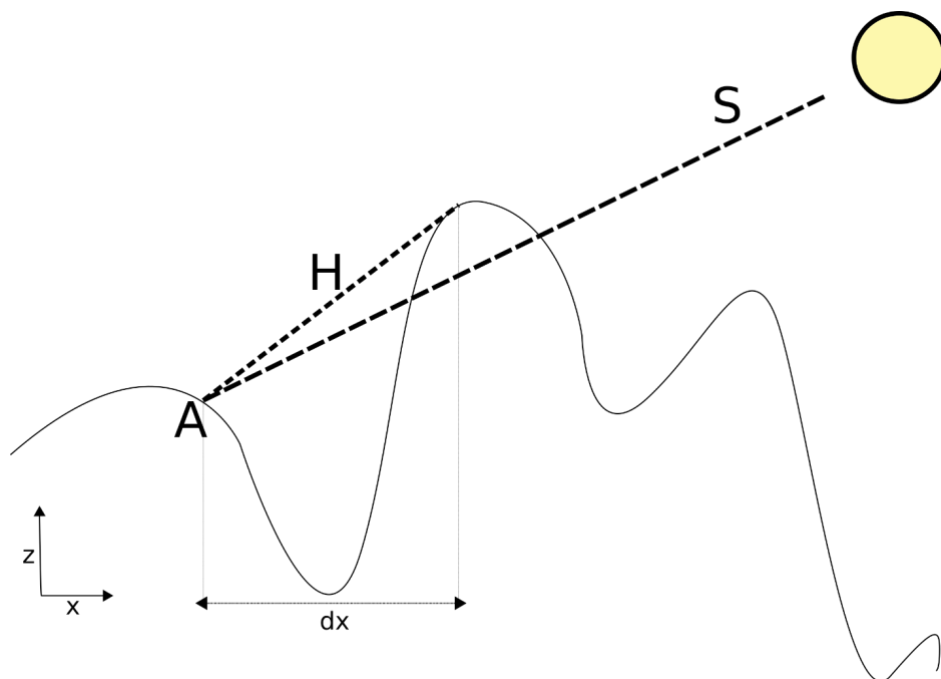




Figure 5: Marmot Creek Research Basin, Kananaskis Valley, Alberta in the Canadian Rocky Mountains. The basin outline is given as solid black, 100 m contour lines shown in brown, stream channels shown in blue, and man-made clearings shown as hatched areas. The meteorological stations used for this study are shown as crosses. The southern-most set of clearings is the Nakiska Ski Resort.)



5

Figure 6: Dozier and Frew (1990) horizon shadowing algorithm. For observer A , a search along the azimuth that corresponds to the solar vector S is performed such that if the slope of H is greater than that of S , A is in shadow.

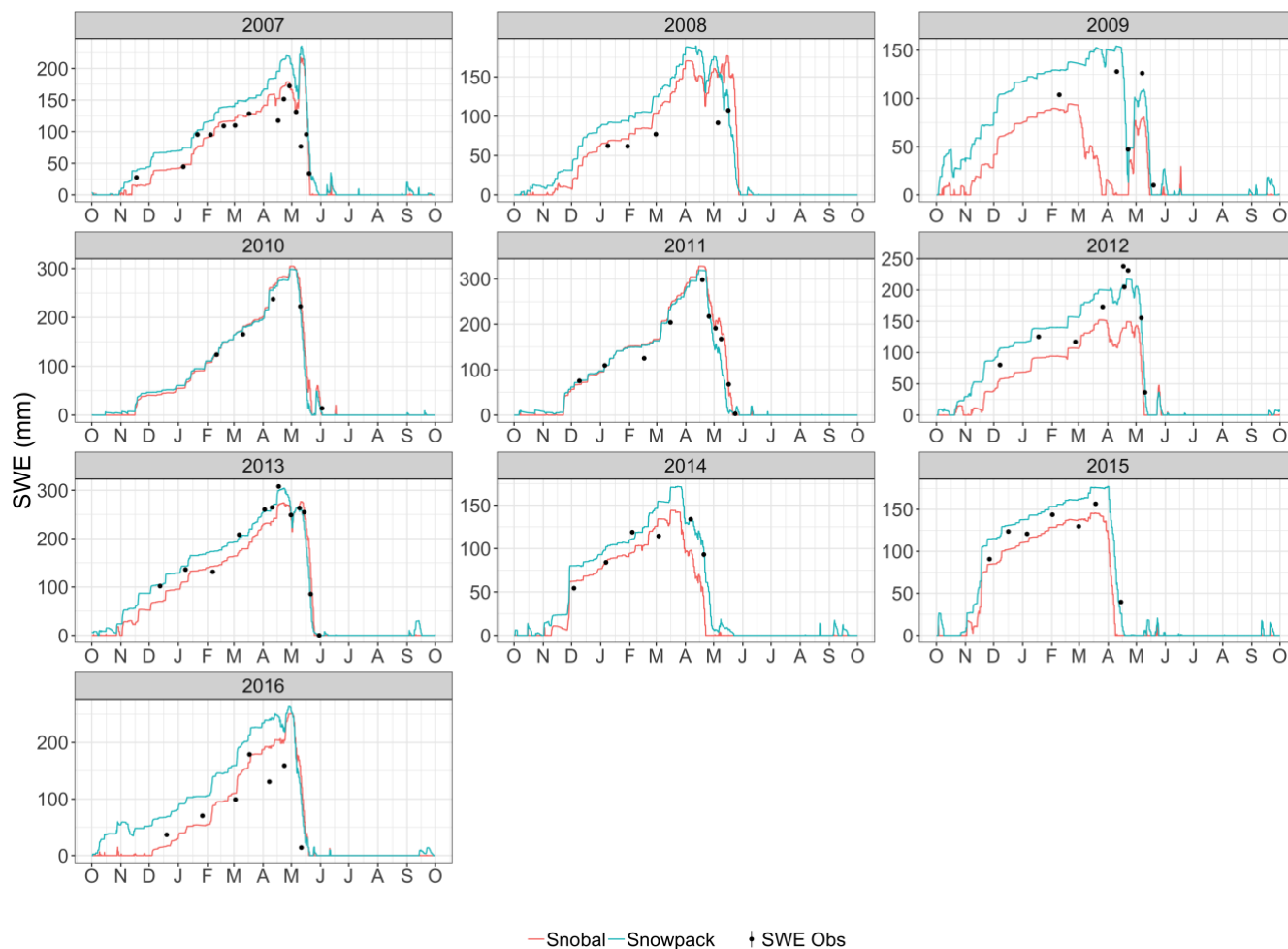


Figure 7: Comparison of Snobal (red) and Snowpack (blue) run as a point simulation within CHM for the Upper Clearing site at Marmot Creek Research Basin for 10 hydrological years. Manual snowcourse observations are shown as black dots with 10% uncertainty (vertical line within dot).

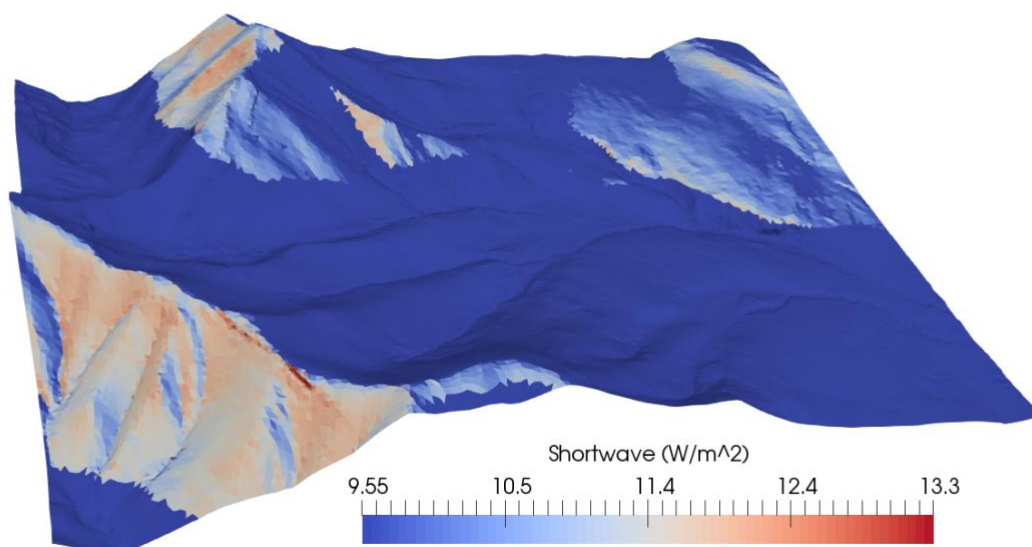


Figure 8: Incoming shortwave radiation for the Marmot Creek Research Basin for 2011-02-01 17:00 local time. The shadowing algorithm of Dozier and Frew (1990) (DF90) has been implemented on the unstructured mesh. Uniform dark blue are shadowed areas.

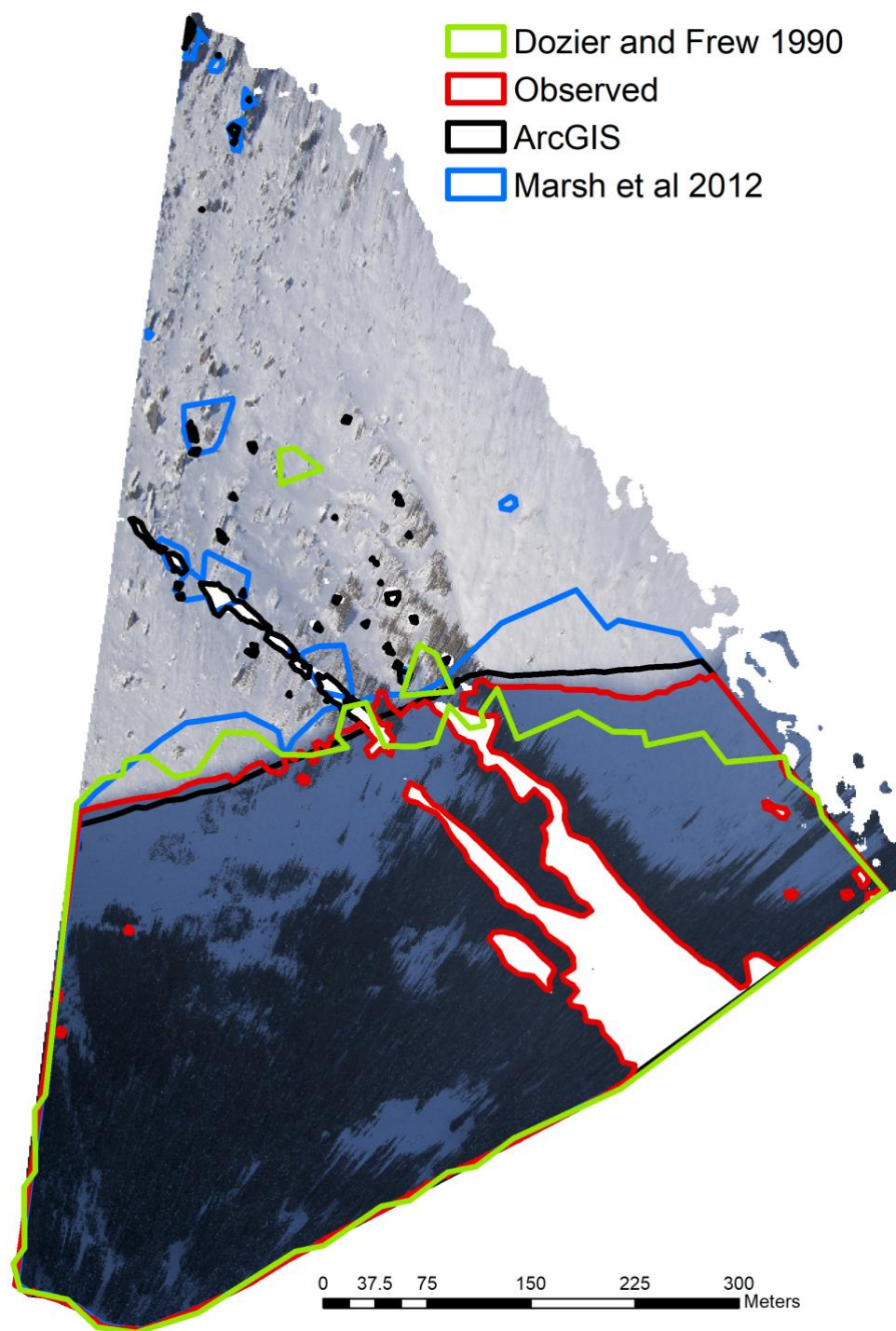
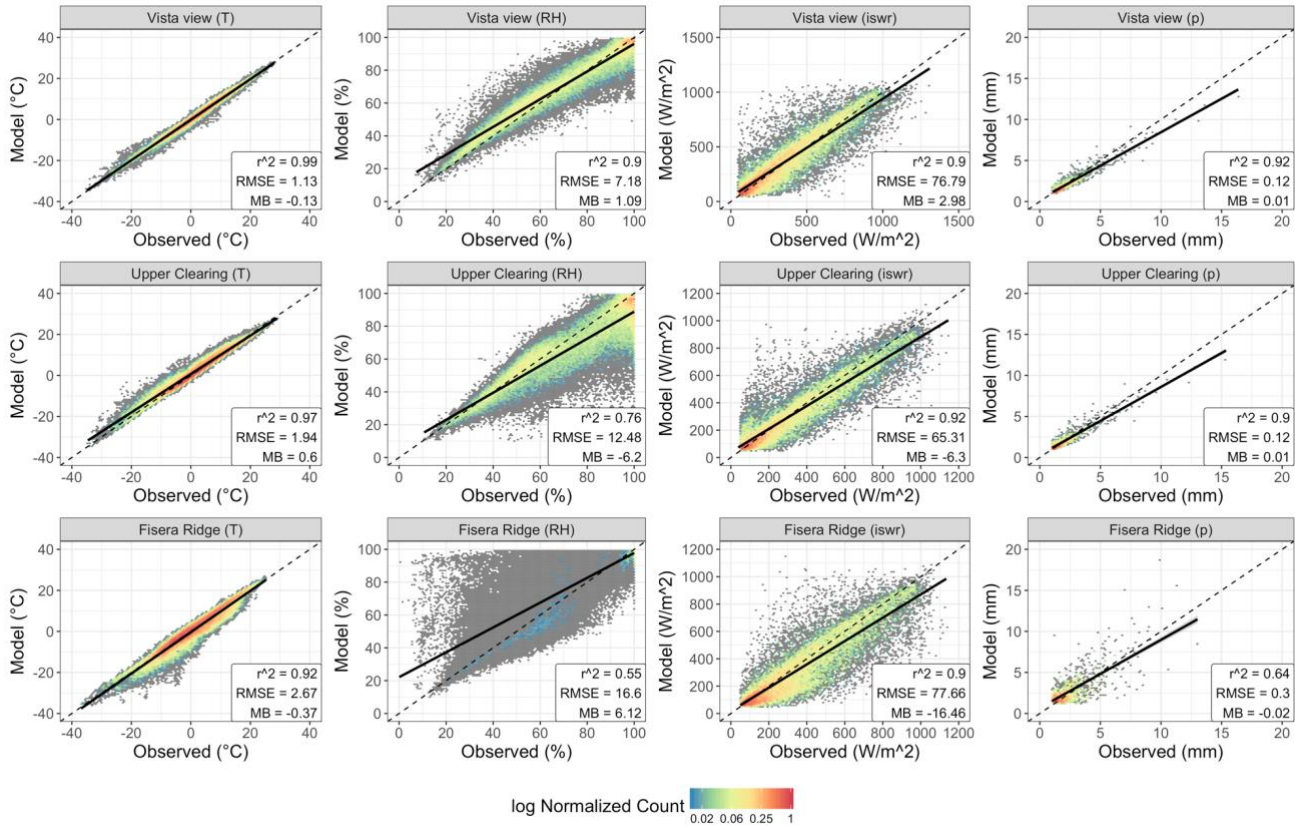




Figure 9: This shows an orthorectified terrestrial photo of a shadow passing over Mt. Collembola from Fisera Ridge – details are found in Marsh et al. (2012). The location of the shadowed region for 2011-02-01 17:00 local time is shown for the DF90 algorithm described herein (green), the observed shadow (red), the ArcGIS implementation for a 1m x 1m LiDAR raster (black), and for the Marsh et al. (2012) algorithm (blue).



5

Figure 10: Leave one out analysis for Vista View (top row), Upper Clearing (middle), and Fisera Ridge (bottom). The values have been binned into 100 hex-bins and coloured using the log of the normalized per-bin count. Grey values are bins that have a normalized count of less than 0.01.

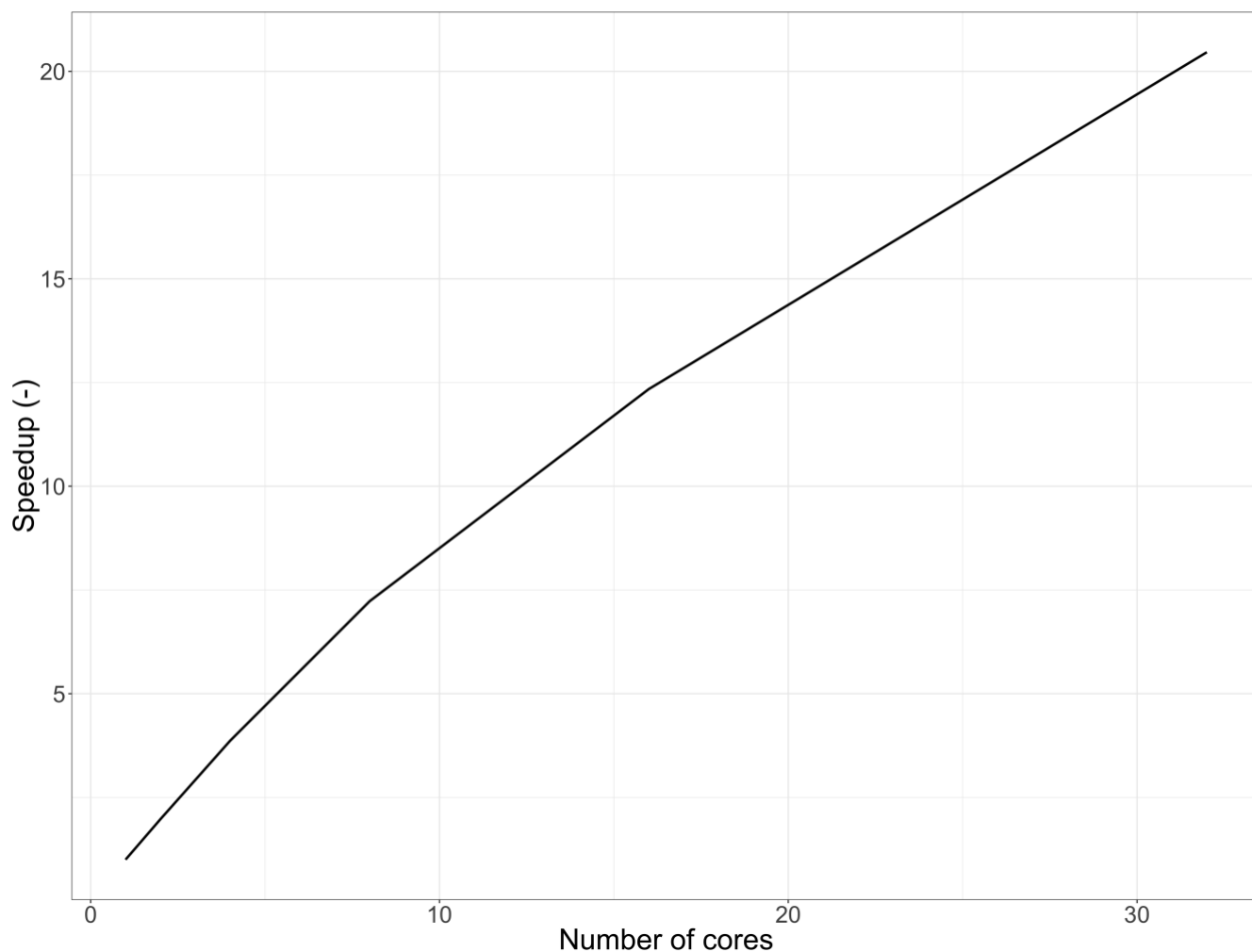


Figure 11: Speedup for a $\approx 100,000$ triangle mesh using 1, 2, 4, 6, 8, 16, and 32 cores.

12 — Tables

Table 1: Cold regions surface process representations currently available in CHM

Process	Type/name
Canopy	Open/forest (exp/log) (Ellis et al., 2010; Pomeroy et al., 1998)
Snowpack	2-layer Snobal (Marks et al., 1999); Multi-layer Snowpack (Bartelt and Lehning, 2002); Various



albedo e.g., CLASS (Verseghy, 1991)

Soil Frozen soil infiltration (Gray et al., 2001)

Snow mass redistribution PBSM3D (Marsh et al. (2019), in review); Snowslide (Bernhardt and Schulz, 2010)



Table 2: List of available meteorology interpolants.

Variable	Type
Air temperature	Linear lapse rates (measured, seasonal, constant, neutral stability) (Cullen and Marshall, 2011; Dodson and Marks, 1997; Kunkel, 1989)
Relative humidity	Linear lapse rates (measured, seasonal, constant)(Kunkel, 1989)
Horizontal wind	Topographic curvature (Liston and Elder, 2006); Mason-Sykes (Mason and Sykes, 1979); Uniform wind
Precipitation	Elevation based lapse (Thornton et al., 1997)
Precipitation Phase	Linear; Psychometric (Harder and Pomeroy, 2013); Threshold
Solar radiation	Terrain shadows (Dozier and Frew, 1990; Marsh et al., 2012); Clear sky transmittance (Burridge and Gadd, 1975); Transmittance from observations; Cloud fraction estimates (Walcek, 1994); Direct/diffuse splitting (Iqbal, 1980)
Longwave	T, RH based (Sicart et al., 2006); Constant (Marty et al., 2002)



Table 3: Root mean squared error (RMSE [mm]) and Mean bias (MB [mm]) for the Snowpack and Snobal models at the Upper Clearing site, for each water year.

Year	Snobal RMSE (mm)	Snowpack RMSE (mm)	Snobal MB (mm)	Snowpack MB (mm)
2007	40.7	56.73	18.24	45.56
2008	42.47	42.42	33.65	38.15
2009	65.07	23.22	-49.54	-1.494
2010	20.55	11.24	10.81	3.94
2011	24.18	32.43	15.07	-7.578
2012	57.12	22.26	-49.05	6.92
2013	27.21	15.51	-9.591	-0.04449
2014	28.81	21.12	-13.6	13.69
2015	19.19	19.41	-13.54	13.84
2016	55.55	66.87	27.08	60.7



References

- Ahrens, J., Geveci, B. and Law, C.: ParaView: An End-User Tool for Large Data Visualization, in Visualization handbook, Elsevier, 2005.
- Avanzi, F., Michele, C. D., Morin, S., Carmagnola, C. M. and Lejeune, Y.: Model complexity and data requirements in snow hydrology : seeking a balance in practical applications, doi:10.1002/hyp.10782, 2016.
- 5 Bahremand, A.: HESS Opinions: Advocating process modeling and de-emphasizing parameter estimation, Hydrology and Earth System Sciences Discussions, 12, 12377–12393, doi:10.5194/hessd-12-12377-2015, 2015.
- Bartelt, P. and Lehning, M.: A physical SNOWPACK model for the Swiss avalanche warning Part I: numerical model, Cold Regions Science and Technology, 35, 123–145, doi:10.1016/S0165-232X(02)00074-5, 2002.
- 10 Bavay, M. and Egger, T.: MeteoIO 2.4.2: a preprocessing library for meteorological data, Geoscientific Model Development, 7, 3135–3151, doi:10.5194/gmd-7-3135-2014, 2014.
- Bentley, J. L.: Multidimensional binary search trees used for associative searching, arXiv.org, 18, 509–517, doi:10.1145/361002.361007, 1975.
- Bernhardt, M. and Schulz, K.: SnowSlide: A simple routine for calculating gravitational snow transport, Geophysical Research Letters, 37, n/a–n/a, doi:10.1029/2010gl043086, 2010.
- 15 Beven, K.: Changing ideas in hydrology — The case of physically-based models, Journal of Hydrology, 105, 157–172, doi:10.1016/0022-1694(89)90101-7, 1989.
- Beven, K.: Prophecy, reality and uncertainty in distributed hydrological modelling, Advances in Water Resources, 16, 41–51, doi:10.1016/0309-1708(93)90028-e, 1993.
- 20 Beven, K.: A manifesto for the equifinality thesis, Water Resources Research, 32, 18–36, doi:10.1016/j.jhydrol.2005.07.007, 2006.
- Beven, K. and Westerberg, I.: On red herrings and real herrings: Disinformation and information in hydrological inference, Hydrological Processes, 25, 1676–1680, doi:10.1002/hyp.7963, 2011.
- Binley, A., Elgy, J. and Beven, K.: A physically based model of heterogeneous hillslopes: 1. Runoff production, Water Resources Research, 25, 1219–1226, doi:10.1029/wr025i006p01219, 1989.
- 25 Blöschl, G. and Sivapalan, M.: Scale issues in hydrological modelling: A review, Hydrological Processes, 9, 251–290, doi:10.1002/hyp.3360090305, 1995.



- Bowling, L. C., Pomeroy, J. W. and Lettenmaier, D. P.: Parameterization of Blowing-Snow Sublimation in a Macroscale Hydrology Model, *Journal of Hydrometeorology*, 5, 745–762, doi:10.1175/1525-7541(2004)005<0745:pobsia>2.0.co;2, 2004.
- Brigode, P., Oudin, L. and Perrin, C.: Hydrological model parameter instability: A source of additional uncertainty in estimating the hydrological impacts of climate change?, *Water Resources Research*, 47, 410–425, doi:10.1016/j.jhydrol.2012.11.012, 2013.
- Bring, A., Fedorova, I., Dibike, Y., Hinzman, L., Mård, J., Mernild, S. H., Prowse, T., Semenova, O., Stuefer, S. L. and Woo, M.: Arctic terrestrial hydrology: A synthesis of processes, regional effects, and research challenges, *Journal of Geophysical Research: Biogeosciences*, 121, 621–649, doi:10.1002/2015jg003131, 2016.
- 10 Burridge, D. M. and Gadd, A. J.: The Meteorological Office Operational 10-level Numerical Weather Prediction Model., 1975.
- Bühler, Y., Adams, M. S., Bösch, R. and Stoffel, A.: Mapping snow depth in alpine terrain with unmanned aerial systems (UASs): potential and limitations, *The Cryosphere*, 10, 1075–1088, doi:10.5194/tc-10-1075-2016, 2016.
- Carey, S. K. and Woo, M.-k.: Snowmelt Hydrology of Two Subarctic Slopes, Southern Yukon, Canada Paper Presented at the 11th Northern Res. Basins Symposium/Workshop (Prudhoe Bay to Fairbanks, Alaska, USA – Aug. 18-22, 1997), *Hydrology Research*, 29, 331–346, doi:10.2166/nh.1998.0022, 1998.
- 15 Chang, K.-t.: *Introduction to Geographic Information Systems*, New York, New York, USA., 2008.
- Cherkauer, K. a, Bowling, L. C. and Lettenmaier, D. P.: Variable infiltration capacity cold land process model updates, *Global and Planetary Change*, 38, 151–159, doi:10.1016/s0921-8181(03)00025-0, 2003.
- 20 Clark, M. P., Slater, A. G., Rupp, D. E., Woods, R. A., Vrugt, J. A., Gupta, H. V., Wagener, T. and Hay, L. E.: Framework for Understanding Structural Errors (FUSE): A modular framework to diagnose differences between hydrological models, *Water Resources Research*, 44, n/a–n/a, doi:10.1029/2007wr006735, 2008.
- Clark, M. P., Kavetski, D. and Fenicia, F.: Pursuing the method of multiple working hypotheses for hydrological modeling, *Water Resources Research*, 47, doi:10.1029/2010wr009827, 2011.
- 25 Clark, M. P., Nijssen, B., Lundquist, J. D., Kavetski, D., Rupp, D. E., Woods, R. A., Freer, J. E., Gutmann, E. D., Wood, A. W., Brekke, L. D., Arnold, J. R., Gochis, D. J. and Rasmussen, R. M.: A unified approach for process-based hydrologic modeling: 1. Modeling concept, *Water Resources Research*, 51, 2498–2514, doi:10.1002/2015wr017198, 2015.
- Clark, M. P., Bierkens, M. F. P., Samaniego, L., Woods, R. A., Uijlenhoet, R., Bennett, K. E., Pauwels, V. R. N., Cai, X., Wood, A. W. and Peters-Lidard, C. D.: The evolution of process-based hydrologic models: historical challenges and the



- collective quest for physical realism, *Hydrology and Earth System Sciences*, 21, 3427–3440, doi:10.5194/hess-21-3427-2017, 2017.
- Corripio, J. G.: Snow surface albedo estimation using terrestrial photography, *International Journal of Remote Sensing*, 25, 5705–5729, doi:10.1080/01431160410001709002, 2004.
- 5 Côté, J., Gravel, S., Méthot, A., Patoine, A., Roch, M. and Staniforth, A.: The Operational CMC–MRB Global Environmental Multiscale (GEM) Model. Part I: Design Considerations and Formulation, *Monthly Weather Review*, 126, 1373–1395, doi:10.1175/1520-0493(1998)126<1373:tocmge>2.0.co;2, 1998.
- Cullen, R. M. and Marshall, S. J.: Mesoscale Temperature Patterns in the Rocky Mountains and Foothills Region of Southern Alberta, *Atmosphere-Ocean*, 49, 189–205, doi:10.1080/07055900.2011.592130, 2011.
- 10 Das, T., Bárdossy, A., Zehe, E. and He, Y.: Comparison of conceptual model performance using different representations of spatial variability, *Water Resources Research*, 356, 106–118, doi:10.1016/j.jhydrol.2008.04.008, 2008.
- Davies, T. D., Brimblecombe, P., Tranter, M., Tsiouris, S., Vincent, C. E., Abrahams, P. and Blackwood, I. L.: Seasonal Snowcovers: Physics, Chemistry, Hydrology, in *Seasonal snowcovers: Physics, chemistry, hydrology*, edited by W. J. O.-T. and H. G. Jones, pp. 337–392, D. Reidel Publishing Company, Dordrecht, Holland., 1987.
- 15 DeBeer, C. M., Wheeler, H. S., Quinton, W. L., Carey, S. K., Stewart, R. E., MacKay, M. D. and Marsh, P.: The Changing Cold Regions Network: Observation, diagnosis and prediction of environmental change in the Saskatchewan and Mackenzie River Basins, Canada, *Science China Earth Sciences*, 58, 46–60, doi:10.1007/s11430-014-5001-6, 2015.
- DeBeer, C. M. and Pomeroy, J. W.: Modelling snow melt and snowcover depletion in a small alpine cirque, *Canadian Rocky Mountains, Hydrological Processes*, 23, 2584–2599, doi:10.1002/hyp.7346, 2009.
- 20 Dodson, R. and Marks, D.: Daily air temperature interpolated at high spatial resolution over a large mountainous region, *Climate Research*, 8, 1–20, doi:10.3354/cr008001, 1997.
- Dornes, P., Pomeroy, J. W., Pietroniro, A. and Verseghy, D. L.: Effects of Spatial Aggregation of Initial Conditions and Forcing Data on Modeling Snowmelt Using a Land Surface Scheme, *Journal of Hydrometeorology*, 9, 789–803, doi:10.1175/2007jhm958.1, 2008a.
- 25 Dornes, P. F., Pomeroy, J. W., Pietroniro, A., Carey, S. K. and Quinton, W. L.: Influence of landscape aggregation in modelling snow-cover ablation and snowmelt runoff in a sub-arctic mountainous environment, *Hydrological Sciences Journal*, 53, 725–740, doi:10.1623/hysj.53.4.725, 2008b.
- Dozier, J. and Frew, J.: Rapid calculation of terrain parameters for radiation modeling from digital elevation data, *IEEE Transactions on Geoscience and Remote Sensing*, 28, 963–969, doi:10.1109/36.58986, 1990.



- Duarte, C. M., Lenton, T. M., Wadhams, P. and Wassmann, P.: Abrupt climate change in the Arctic, *Nature Climate Change*, 2, 60–62, doi:10.1038/nclimate1386, 2012.
- E, O. T.: *A guide to NumPy.*, 2006.
- Ellis, C., Pomeroy, J. W., Brown, T. and MacDonald, J.: Simulation of snow accumulation and melt in needleleaf forest environments, *Hydrology and Earth System Sciences*, 14, 925–940, doi:10.5194/hess-14-925-2010, 2010.
- 5 Endrizzi, S., Gruber, S., Dall’Amico, M. and Rigon, R.: GEOTop 2.0: simulating the combined energy and water balance at and below the land surface accounting for soil freezing, snow cover and terrain effects, *Geoscientific Model Development*, 7, 2831–2857, doi:10.5194/gmd-7-2831-2014, 2014.
- Essery, R.: A factorial snowpack model (FSM 1.0), *Geoscientific Model Development*, 8, 3867–3876, doi:10.5194/gmd-8-3867-2015, 2015.
- 10 Essery, R., Li, L. and Pomeroy, J.: A distributed model of blowing snow over complex terrain, *Hydrological Processes*, 13, 2423–2438, doi:10.1002/(sici)1099-1085(199910)13:14:15<2423::aid-hyp853>3.0.co;2-u, 1999.
- Essery, R., Rutter, N., Pomeroy, J., Baxter, R., hli, M. S. a, Gustafsson, D., Barr, A., Bartlett, P. and Elder, E.: SNOWMIP2: An evaluation of forest snow process simulations, *Bulletin of the American Meteorological Society*, 90, 1120–1135, doi:10.1175/2009bams2629.1, 2009.
- 15 Essery, R., Morin, S., Lejeune, Y. and Ménard, C. B.: A comparison of 1701 snow models using observations from an alpine site, *Advances in Water Resources*, 55, 131–148, doi:10.1016/j.advwatres.2012.07.013, 2013.
- Etchevers, P., Martin, E., Brown, R., Fierz, C., Lejeune, Y., Bazile, E., Boone, A., Dai, Y.-J., Essery, R., Fernandez, A., Gusev, Y., Jordan, R., Koren, V., Kowalczyk, E., Nasonova, N. O., Pyles, R. D., Schlosser, A., Shmakina, A. B., Smirnova, T. G., Strasser, U., Verseghy, D., Yamazaki, T. and Yang, Z.-L.: Validation of the energy budget of an alpine snowpack simulated by several snow models (SnowMIP project), *Annals of Glaciology*, 38, 150–158, doi:10.3189/172756404781814825, 2004.
- Fang, X., Pomeroy, J. W., Ellis, C. R., MacDonald, M. K., DeBeer, C. M. and Brown, T.: Multi-variable evaluation of hydrological model predictions for a headwater basin in the Canadian Rocky Mountains, *Hydrology and Earth System Sciences*, 17, 1635–1659, doi:10.5194/hess-17-1635-2013, 2013.
- 25 Fang, X., Pomeroy, J. W., DeBeer, C. M., Harder, P. and Siemens, E.: Hydrometeorological data from Marmot Creek Research Basin, Canadian Rockies, *Earth System Science Data*, 11, 455–471, doi:10.5194/essd-11-455-2019, 2019.
- Fatichi, S., Vivoni, E. R., Ogden, F. L., Ivanov, V. Y., Mirus, B., Gochis, D., Downer, C. W., Camporese, M., Davison, J. H., Ebel, B., Jones, N., Kim, J., Mascaro, G., Niswonger, R., Restrepo, P., Rigon, R., Shen, C., Sulis, M. and Tarboton, D.:



- An overview of current applications, challenges, and future trends in distributed process-based models in hydrology, *Journal of Hydrology*, 537, 45–60, doi:<http://dx.doi.org/10.1016/j.jhydrol.2016.03.026>, 2016.
- Fenicia, F., Kavetski, D. and Savenije, H. H. G.: Elements of a flexible approach for conceptual hydrological modeling: 1. Motivation and theoretical development, *Water Resources Research*, 47, n/a–n/a, doi:[10.1029/2010wr010174](https://doi.org/10.1029/2010wr010174), 2011.
- 5 Fiddes, J. and Gruber, S.: TopoSCALE v.1.0: downscaling gridded climate data in complex terrain, *Geoscientific Model Development*, 7, 387–405, doi:[10.5194/gmd-7-387-2014](https://doi.org/10.5194/gmd-7-387-2014), 2014.
- Freeze, R. A.: Streamflow generation, *Reviews of Geophysics*, 12, 627–647, doi:[10.1029/rg012i004p00627](https://doi.org/10.1029/rg012i004p00627), 1974.
- Freeze, R. A. and Harlan, R. L.: Blueprint for a physically-based, digitally-simulated hydrologic response model, *Journal of Hydrology*, 9, 237–258, doi:[10.1016/0022-1694\(69\)90020-1](https://doi.org/10.1016/0022-1694(69)90020-1), 1969.
- 10 Fu, P. and Rich, P. M.: Design and implementation of the Solar Analyst: an ArcView extension for modeling solar radiation at landscape scales, p. 1–33, San Diego, USA., 1999.
- Gelfan, A. N., Pomeroy, J. W. and Kuchment, L. S.: Modeling Forest Cover Influences on Snow Accumulation, Sublimation, and Melt, *Journal of Hydrometeorology*, 5, 785–803, doi:[10.1175/1525-7541\(2004\)005<0785:mfcios>2.0.co;2](https://doi.org/10.1175/1525-7541(2004)005<0785:mfcios>2.0.co;2), 2004.
- 15 Golding, D. L.: Research results from Marmot Creek experimental watershed, Alberta, Canada, p. 397–404, Wellington, New Zealand., 1970.
- Gray, D. M. and Male, D. H.: *Handbook of Snow: Principles, Processes, Management, and Use*, Toronto, Canada., 1981.
- Gray, D. M., Toth, B., Zhao, L., Pomeroy, J. W. and Granger, R. J.: Estimating areal snowmelt infiltration into frozen soils, *Hydrological Processes*, 15, 3095–3111, doi:[10.1002/hyp.320](https://doi.org/10.1002/hyp.320), 2001.
- 20 Harder, P. and Pomeroy, J.: Estimating precipitation phase using a psychrometric energy balance method, *Hydrological Processes*, 27, 1901–1914, doi:[10.1002/hyp.9799](https://doi.org/10.1002/hyp.9799), 2013.
- Harder, P., Schirmer, M., Pomeroy, J. and Helgason, W.: Accuracy of snow depth estimation in mountain and prairie environments by an unmanned aerial vehicle, *The Cryosphere*, 10, 2559–2571, doi:[10.5194/tc-10-2559-2016](https://doi.org/10.5194/tc-10-2559-2016), 2016.
- Harder, P., Pomeroy, J. W. and Helgason, W. D.: A simple model for local-scale sensible and latent heat advection contributions to snowmelt, *Hydrology and Earth System Sciences*, 23, 1–17, doi:[10.5194/hess-23-1-2019](https://doi.org/10.5194/hess-23-1-2019), 2019.
- 25 Hedstrom, N. R. and Pomeroy, J. W.: Measurements and modelling of snow interception in the boreal forest, *Hydrological Processes*, 12, 1611–1625, doi:[10.1002/\(sici\)1099-1085\(199808/09\)12:10/11<1611::aid-hyp684>3.0.co;2-4](https://doi.org/10.1002/(sici)1099-1085(199808/09)12:10/11<1611::aid-hyp684>3.0.co;2-4), 1998.



- Hopkinson, C., Crasto, N., Marsh, P., Forbes, D. and Lesack, L.: Investigating the spatial distribution of water levels in the Mackenzie Delta using airborne LiDAR, *Hydrological Processes*, 25, 2995–3011, doi:10.1002/hyp.8167, 2011.
- Horne, F. E. and Kavvas, M. L.: Physics of the spatially averaged snowmelt process, *Journal of Hydrology*, 191, 179–207, doi:10.1016/s0022-1694(96)03063-6, 1997.
- 5 Hrachowitz, M. and Clark, M. P.: HESS Opinions: The complementary merits of competing modelling philosophies in hydrology, *Hydrology and Earth System Sciences*, 21, 3953–3973, doi:10.5194/hess-21-3953-2017, 2017.
- Hubbard, S. S., Gangodagamage, C., Dafflon, B., Wainwright, H., Peterson, J., Gusmeroli, A., Ulrich, C., Wu, Y., Wilson, C., Rowland, J., Tweedie, C. and Wulschleger, S. D.: Quantifying and relating land-surface and subsurface variability in permafrost environments using LiDAR and surface geophysical datasets, *Hydrogeology Journal*, 21, 149–169, doi:10.1007/s10040-012-0939-y, 2013.
- 10 Iqbal, M.: Prediction of hourly diffuse solar radiation from measured hourly global radiation on a horizontal surface, *Solar Energy*, 24, 491–503, doi:10.1016/0038-092x(80)90317-5, 1980.
- Ivanov, V., Vivoni, E., Bras, R. and Entekhabi, D.: Preserving high-resolution surface and rainfall data in operational-scale basin hydrology: a fully-distributed physically-based approach, *Water Resources Research*, 298, 80–111, doi:10.1016/j.jhydrol.2004.03.041, 2004.
- 15 Jones, E., Oliphant, T. and Peterson, P.: *SciPy: Open Source Scientific Tools for Python.*, 2018.
- Jordan, R.: A one-dimensional temperature model for a snow cover. Technical documentation for SN THERM.89., 1991.
- Klemeš, V.: Conceptualization and scale in hydrology, *Journal of Hydrology*, 65, 1–23, doi:10.1016/0022-1694(83)90208-1, 1983.
- 20 Kuchment, L. and Gelfan, A.: Physicomathematical model of snow accumulation and melt in a forest, *Russian Meteorology and Hydrology*, 57—65, 2004.
- Kumar, M., Marks, D., Dozier, J., Reba, M. and Winstral, A.: Evaluation of distributed hydrologic impacts of temperature-index and energy-based snow models, *Advances in Water Resources*, 56, 77–89, doi:10.1016/j.advwatres.2013.03.006, 2013.
- Kunkel, K. E.: Simple procedures for extrapolation of humidity variables in the mountainous western United States, *Journal of Climate*, 2, 656–669, 1989.
- 25 Lafaysse, M., Cluzet, B., Dumont, M., Lejeune, Y., Vionnet, V. and Morin, S.: A multiphysical ensemble system of numerical snow modelling, *Cryosphere*, 11, 1173–1198, doi:10.5194/tc-11-1173-2017, 2017.
- Latifovic, R. and Pouliot, D.: Analysis of climate change impacts on lake ice phenology in Canada using the historical satellite data record, *Remote Sensing of Environment*, 106, 492–507, doi:10.1016/j.rse.2006.09.015, 2007.



- Leavesley, G. H., Markstrom, S. L., Restrepo, P. J. and Viger, R. J.: A modular approach to addressing model design, scale, and parameter estimation issues in distributed hydrological modelling, *Hydrological Processes*, 16, 173–187, doi:10.1002/hyp.344, 2002.
- Lehning, M., Bartelt, P., Brown, B., Fierz, C. and Satyawali, P.: A physical SNOWPACK model for the Swiss avalanche warning Part II. Snow microstructure, *Cold Regions Science and Technology*, 35, 147–167, doi:10.1016/s0165-232x(02)00073-3, 2002.
- Lehning, M., Völksch, I., Gustafsson, D., Nguyen, T. A., Stähli, M. and Zappa, M.: ALPINE3D: a detailed model of mountain surface processes and its application to snow hydrology, *Hydrological Processes*, 20, 2111–2128, doi:10.1002/hyp.6204, 2006.
- 10 Lehning, M., Löwe, H., Ryser, M. and Raderschall, N.: Inhomogeneous precipitation distribution and snow transport in steep terrain, *Water Resources Research*, 44, doi:10.1029/2007wr006545, 2008.
- Leroux, N. R. and Pomeroy, J. W.: Modelling capillary hysteresis effects on preferential flow through melting and cold layered snowpacks, *Advances in Water Resources*, 107, 250–264, doi:10.1016/j.advwatres.2017.06.024, 2017.
- Liston, G. E. and Elder, K.: A Meteorological Distribution System for High-Resolution Terrestrial Modeling (MicroMet),
15 *Journal of Hydrometeorology*, 7, 217–234, doi:10.1175/jhm486.1, 2006.
- Lundberg, A., Ala-Aho, P., Eklo, O., Klöve, B., Kværner, J. and Stumpp, C.: Snow and frost: implications for spatiotemporal infiltration patterns – a review, *Hydrological Processes*, 30, 1230–1250, doi:10.1002/hyp.10703, 2016.
- MacDonald, M. K., Pomeroy, J. W. and Pietroniro, A.: Parameterizing redistribution and sublimation of blowing snow for hydrological models: tests in a mountainous subarctic catchment, *Hydrological Processes*, 23, 2570–2583,
20 doi:10.1002/hyp.7356, 2009.
- Marks, D., Dozier, J. and Davis, R. E.: Climate and energy exchange at the snow surface in the Alpine Region of the Sierra Nevada: 1. Meteorological measurements and monitoring, *Water Resources Research*, 28, 3029–3042, doi:10.1029/92wr01482, 1992.
- Marks, D., Kimball, J., Tingey, D. and Link, T.: The sensitivity of snowmelt processes to climate conditions and forest cover
25 during rain-on-snow: a case study of the 1996 Pacific Northwest flood, *Hydrological Processes*, 12, 1569–1587, doi:10.1002/(sici)1099-1085(199808/09)12:10/11<1569::aid-hyp682>3.0.co;2-1, 1998.
- Marks, D., Domingo, J., Susong, D., Link, T. and Garen, D.: A spatially distributed energy balance snowmelt model for application in mountain basins, *Hydrological Processes*, 13, 1935–1959, doi:10.1002/(sici)1099-1085(199909)13:12/13<1935::aid-hyp868>3.0.co;2-c, 1999.



- Marks, D., Winstral, A., Reba, M., Pomeroy, J. and Kumar, M.: An evaluation of methods for determining during-storm precipitation phase and the rain/snow transition elevation at the surface in a mountain basin, *Advances in Water Resources*, 55, 98–110, doi:10.1016/j.advwatres.2012.11.012, 2013.
- Marsh, C. B., Pomeroy, J. W. and Spiteri, R. J.: Implications of mountain shading on calculating energy for snowmelt using unstructured triangular meshes, *Hydrological Processes*, 26, 1767–1778, doi:10.1002/hyp.9329, 2012.
- Marsh, C. B., Spiteri, R. J., Pomeroy, J. W. and Wheeler, H. S.: Multi-objective unstructured triangular mesh generation for use in hydrological and land surface models, *Computers & Geosciences*, 119, 49–67, doi:10.1016/j.cageo.2018.06.009, 2018.
- Marsh, C. B., Pomeroy, J. W., Spiteri, R. J. and Wheeler, H. S.: A finite volume blowing snow model for use with variable resolution meshes, *Water Resources Research*, 2019.
- 10 Marty, C., Philipona, R., Fröhlich, C. and Ohmura, A.: Altitude dependence of surface radiation fluxes and cloud forcing in the alps: results from the alpine surface radiation budget network, *Theoretical and Applied Climatology*, 72, 137–155, doi:10.1007/s007040200019, 2002.
- Mason, P. and Sykes, R.: Flow over an isolated hill of moderate slope, *Quarterly Journal of the Royal Meteorological Society*, 105, 383–395, doi:10.1002/qj.49710544405, 1979.
- 15 Maxwell, R. M. and Kollet, S. J.: Interdependence of groundwater dynamics and land-energy feedbacks under climate change, *Nature Geoscience*, 1, 665–669, doi:10.1038/ngeo315, 2008.
- McCauley, C. a, White, D. M., Lilly, M. R. and Nyman, D. M.: A comparison of hydraulic conductivities, permeabilities and infiltration rates in frozen and unfrozen soils, *Cold Regions Science and Technology*, 34, 117–125, doi:10.1016/s0165-232x(01)00064-7, 2002.
- 20 Mendoza, P. A., Clark, M. P., Barlage, M., Rajagopalan, B., Samaniego, L., Abramowitz, G. and Gupta, H.: Are we unnecessarily constraining the agility of complex process-based models?, *Water Resources Research*, 51, 716–728, doi:10.1002/2014wr015820, 2015.
- Michlmayr, G., Lehning, M., Kobltschnig, G., Holzmann, H., Zappa, M., Mott, R. and Schöner, W.: Application of the Alpine 3D model for glacier mass balance and glacier runoff studies at Goldbergkees, Austria, *Hydrological Processes*, 22, 3941–3949, doi:10.1002/hyp.7102, 2008.
- 25 Milly, P. C. D., Betancourt, J., Falkenmark, M., Hirsch, R. M., Kundzewicz, Z., Lettenmaier, D. P. and Stouffer, R. J.: Stationarity Is Dead: Whither Water Management?, *2Science*, 319, 573–574, 2008.
- Mohanty, B. P.: Soil Hydraulic Property Estimation Using Remote Sensing: A Review, *Vadose Zone Journal*, 12, 0, doi:10.2136/vzj2013.06.0100, 2013.



- Mosier, T. M., Hill, D. F. and Sharp, K. V.: How Much Cryosphere Model Complexity is Just Right? Exploration Using the Conceptual Cryosphere Hydrology Framework, *The Cryosphere Discussions*, 1 33, doi:10.5194/tc-2016-17, 2016.
- Mote, P. W., Hamlet, A. F., Clark, M. P. and Lettenmaier, D. P.: Declining Mountain Snowpack in Western North America*, *Bulletin of the American Meteorological Society*, 86, 39 49, doi:10.1175/bams-86-1-39, 2005.
- 5 Mott, R., Schirmer, M., Bavay, M., Grünewald, T. and Lehning, M.: Understanding snow-transport processes shaping the mountain snow-cover, *The Cryosphere*, 4, 545 559, doi:10.5194/tc-4-545-2010, 2010.
- Mott, R., Gromke, C., Grünewald, T. and Lehning, M.: Relative importance of advective heat transport and boundary layer decoupling in the melt dynamics of a patchy snow cover, *Advances in Water Resources*, 55, 88–97, doi:10.1016/j.advwatres.2012.03.001, 2013.
- 10 Munro, D. S. and Young, G. J.: An operational net shortwave radiation model for glacier basins, *Water Resources Research*, 18, 220–230, doi:10.1029/wr018i002p00220, 1982.
- Musselman, K. N., Pomeroy, J. W. and Link, T. E.: Variability in shortwave irradiance caused by forest gaps: Measurements, modelling, and implications for snow energetics, *Agricultural and Forest Meteorology*, 207, 69 82, doi:10.1016/j.agrformet.2015.03.014, 2015.
- 15 Musselman, K. N., Clark, M. P., Liu, C., Ikeda, K. and Rasmussen, R.: Slower snowmelt in a warmer world, *Nature Climate Change*, 7, 214 219, doi:10.1038/nclimate3225, 2017.
- Nazemi, A., Wheeler, H. S., Chun, K. P. and Elshorbagy, A.: A stochastic reconstruction framework for analysis of water resource system vulnerability to climate-induced changes in river flow regime, *Water Resources Research*, 49, 291–305, doi:10.1029/2012wr012755, 2013.
- 20 Olyphant, G. A.: Longwave Radiation in Mountainous Areas and Its Influence on the Energy Balance of Alpine Snowfields, *Water Resources Research*, 22, 62–66, doi:10.1029/wr022i001p00062, 1986.
- Or, D., Lehmann, P. and Assouline, S.: Natural length scales define the range of applicability of the Richards equation for capillary flows, *Water Resources Research*, 51, 7130–7144, doi:10.1002/2015wr017034, 2015.
- Painter, S. L., Coon, E. T., Atchley, A. L., Berndt, M., Garimella, R., Moulton, J. D., Svyatskiy, D. and Wilson, C. J.:
- 25 Integrated surface/subsurface permafrost thermal hydrology: Model formulation and proof-of-concept simulations, *Water Resources Research*, 52, 6062–6077, doi:10.1002/2015wr018427, 2016.
- Paniconi, C. and Putti, M.: Physically based modeling in catchment hydrology at 50: Survey and outlook, *Water Resources Research*, 51, 7090–7129, doi:10.1002/2015wr017780, 2015.



- Perrin, C., Michel, C. and Andréassian, V.: Does a large number of parameters enhance model performance? Comparative assessment of common catchment model structures on 429 catchments, *Journal of Hydrology*, 242, 275–301, doi:10.1016/S0022-1694(00)00393-0, 2001.
- Pietroniro, a, Fortin, V., Kouwen, N., Neal, C., Turcotte, R., Davison, B., Verseghy, D., Soulis, E. D., Caldwell, R., Evora, N. and Pellerin, P.: Development of the MESH modelling system for hydrological ensemble forecasting of the Laurentian Great Lakes at the regional scale, *Hydrology and Earth System Sciences*, 11, 1279–1294, doi:10.5194/hess-11-1279-2007, 2007.
- Pomeroy, J. and Bernhardt, M.: Project Report for the 2017 GEWEX GHP Meeting, Kathmandu, Nepal., 2017.
- Pomeroy, J., Fang, X. and Ellis, C.: Sensitivity of snowmelt hydrology in Marmot Creek, Alberta, to forest cover disturbance, *Hydrological Processes*, 26, 1891–1904, doi:10.1002/hyp.9248, 2012.
- Pomeroy, J. W., Gray, D. M. and Landine, P. G.: The Prairie Blowing Snow Model: characteristics, validation, operation, *Journal of Hydrology*, 144, 165–192, doi:10.1016/0022-1694(93)90171-5, 1993.
- Pomeroy, J. W., Parviainen, J., Hedstrom, N. and Gray, D. M.: Coupled modelling of forest snow interception and sublimation, *Hydrological Processes*, 12, 2317–2337, doi:10.1002/(sici)1099-1085(199812)12:15<2317::aid-hyp799>3.0.co;2-x, 1998.
- Pomeroy, J. W., Toth, B., Granger, R. J., Hedstrom, N. R. and Essery, R. L. H.: Variation in surface energetics during snowmelt in a subarctic mountain catchment, *Journal of Hydrometeorology*, 4, 702–719, doi:10.1175/1525-7541(2003)004<0702:viseds>2.0.co;2, 2003.
- Pomeroy, J. W., Gray, D. M., Brown, T., Hedstrom, N. R., Quinton, W. L., Granger, R. J. and Carey, S. K.: The cold regions hydrological model: a platform for basing process representation and model structure on physical evidence, *Hydrological Processes*, 21, 2650–2667, doi:10.1002/hyp.6787, 2007.
- Pomeroy, J. W., Fang, X., Shook, K. and Whitfield, P. H.: Predicting in ungauged basins using physical principles obtained using the deductive, inductive, and abductive reasoning approach, in *Putting prediction in ungauged basins into practice*, edited by J. W. Pomeroy and P. H. Whitfield, p. 41–62, Canadian Water Resources Association., 2013.
- Raderschall, N., Lehning, M. and Schär, C.: Fine-scale modeling of the boundary layer wind field over steep topography, *Water Resources Research*, 44, 1–18, doi:10.1029/2007wr006544, 2008.
- Raleigh, M. S., Livneh, B., Lapo, K. and Lundquist, J. D.: How does availability of meteorological forcing data impact physically-based snowpack simulations?, *Journal of Hydrometeorology*, 150904104740009, doi:10.1175/jhm-d-14-0235.1, 2015.



- Rasouli, K., Pomeroy, J. W. and Marks, D. G.: Snowpack sensitivity to perturbed climate in a cool mid-latitude mountain catchment, *Hydrological Processes*, 29, 3925–3940, doi:10.1002/hyp.10587, 2015.
- Razavi, S. and Gupta, H. V.: A new framework for comprehensive, robust, and efficient global sensitivity analysis: 1. Theory, *Water Resources Research*, 52, 423–439, doi:10.1002/2015wr017558, 2016.
- 5 Rew, R. and Davis, G.: NetCDF: An Interface for Scientific Data Access, *IEEE Computer Graphics and Applications*, 10, 76–82, doi:10.1109/38.56302, 1990.
- Rothwell, R., Hillman, G. and Pomeroy, J. W.: Marmot Creek Experimental Watershed Study, *Forestry Chronicle*, 92, 32–36, doi:10.5558/tfc2016-010, 2016.
- Rouse, W. R., Oswald, C. J., Binyamin, J., Spence, C., Schertzer, W. M., Blanken, P. D., Bussi eres, N. and Duguay, C. R.:
10 The Role of Northern Lakes in a Regional Energy Balance, *Journal of Hydrometeorology*, 6, 291–305, doi:10.1175/jhm421.1, 2005.
- Samaniego, L., Kumar, R., Thober, S., Rakovec, O., Zink, M., Wanders, N., Eisner, S., Schmied, H. M., Sutanudjaja, E., Warrach-Sagi, K. and Attinger, S.: Toward seamless hydrologic predictions across spatial scales, *Hydrology and Earth System Sciences*, 21, 4323–4346, doi:10.5194/hess-21-4323-2017, 2017.
- 15 Savenije, H. H. G.: HESS Opinions "The art of hydrology", *Hydrology and Earth System Sciences*, 13, 157–161, doi:10.5194/hess-13-157-2009, 2009.
- Schl ogl, S., Lehning, M., Fierz, C. and Mott, R.: Representation of Horizontal Transport Processes in Snowmelt Modeling by Applying a Footprint Approach, *Frontiers in Earth Science*, 6, 120, doi:10.3389/feart.2018.00120, 2018.
- Schroeder, W., Martin, K. and Lorensen, B.: *The Visualization Toolkit*, 4th ed., 2006.
- 20 Shewchuk, J.: Triangle: engineering a 2D quality mesh generator and Delaunay triangulator, in *Applied computational geometry towards geometric engineering*, p. 203–222, Springer Berlin / Heidelberg., 1996.
- Shook, K. and Gray, D. M.: Small-scale Spatial Structure Of Shallow Snowcovers, *Hydrological Processes*, 10, 1283–1292, doi:10.1002/(sici)1099-1085(199610)10:10<1283::aid-hyp460>3.0.co;2-m, 1996.
- Shook, K., Pomeroy, J. and Kamp, G. van der: The transformation of frequency distributions of winter precipitation to spring streamflow probabilities in cold regions; case studies from the Canadian Prairies, *Journal of Hydrology*, 521, 395–409, doi:10.1016/j.jhydrol.2014.12.014, 2015.
- 25 Sicart, J. E., Pomeroy, J. W., Essery, R. L. H. and Bewley, D.: Incoming longwave radiation to melting snow: observations, sensitivity and estimation in Northern environments, *Hydrological Processes*, 20, 3697–3708, doi:10.1002/hyp.6383, 2006.



- Sivapalan, M.: From Engineering Hydrology to Earth System Science : Milestones in the Transformation of Hydrologic Science, *Hydrology and Earth System Sciences Discussions*, 1 47, doi:10.5194/hess-2017-670, 2017.
- Slater, a G., Barrett, a P., Clark, M. P., Lundquist, J. D. and Raleigh, M. S.: Uncertainty in seasonal snow reconstruction: Relative impacts of model forcing and image availability, *Advances in Water Resources*, 55, 165–177, doi:10.1016/j.advwatres.2012.07.006, 2013.
- Smith, C. D.: The relationship between snowfall catch efficiency and wind speed for the Geonor T-200B precipitation gauge utilizing various wind shield configurations., pp. 115–121., 2009.
- Spence, C. and Mengistu, S.: Deployment of an unmanned aerial system to assist in mapping an intermittent stream, *Hydrological Processes*, 30, 493–500, doi:10.1002/hyp.10597, 2016.
- 10 Tangelder, H. and Fabri, A.: dD Spatial Searching, in *CGAL user and reference manual*, CGAL Editorial Board., 2018.
- Thornton, P. E., Running, S. W. and White, M. A.: Generating surfaces of daily meteorological variables over large regions of complex terrain, *Water Resources Research*, 190, 214–251, doi:10.1016/s0022-1694(96)03128-9, 1997.
- Todini, E.: Rainfall-runoff modeling - Past, present and future, *Water Resources Research*, 100, 341–352, doi:10.1016/0022-1694(88)90191-6, 1988.
- 15 Tucker, G.: An object-oriented framework for distributed hydrologic and geomorphic modeling using triangulated irregular networks, *Computers & Geosciences*, 27, 959–973, doi:10.1016/s0098-3004(00)00134-5, 2001.
- Vaze, J., Post, D. a, Chiew, F. H. S., Perraud, J. M., Viney, N. R. and Teng, J.: Climate non-stationarity – Validity of calibrated rainfall-runoff models for use in climate change studies, *Water Resources Research*, 394, 447–457, doi:10.1016/j.jhydrol.2010.09.018, 2010.
- 20 Versegny, D. L.: Class—A Canadian land surface scheme for GCMS. I. Soil model, *International Journal of Climatology*, 11, 111–133, doi:10.1002/joc.3370110202, 1991.
- Versegny, D. L., McFarlane, N. A. and Lazare, M.: Class—A Canadian land surface scheme for GCMS, II. Vegetation model and coupled runs, *International Journal of Climatology*, 13, 347–370, doi:10.1002/joc.3370130402, 1993.
- Vionnet, V., Brun, E., Morin, S., Boone, A., Faroux, S., Moigne, P. L., Martin, E. and Willemet, J. M.: The detailed snowpack scheme Crocus and its implementation in SURFEX v7.2, *Geoscientific Model Development*, 5, 773–791, doi:10.5194/gmd-5-773-2012, 2012.
- 25 Viviroli, D., Dürr, H. H., Messerli, B., Meybeck, M. and Weingartner, R.: Mountains of the world, water towers for humanity: Typology, mapping, and global significance, *Water Resources Research*, 43, 1–13, doi:10.1029/2006wr005653, 2007.



- Vrugt, J. a, Braak, C. J. F. ter, Clark, M. P., Hyman, J. M. and Robinson, B. a: Treatment of input uncertainty in hydrologic modeling: Doing hydrology backward with Markov chain Monte Carlo simulation, *Water Resources Research*, 44, 937, doi:10.1029/2007wr006720, 2008.
- Wagner, T. and Montanari, A.: Convergence of approaches toward reducing uncertainty in predictions in ungauged basins, *Water Resources Research*, 47, W06301, doi:10.1029/2010wr009469, 2011.
- Walcek, C. J.: Cloud cover and its relationship to relative humidity during a springtime midlatitude cyclone, *Monthly Weather Review*, 122, 1021–1035, 1994.
- Walvoord, M. A. and Kurylyk, B. L.: Hydrologic Impacts of Thawing Permafrost—A Review, *Vadose Zone Journal*, 15, doi:10.2136/vzj2016.01.0010, 2016.
- Wayand, N. E., Marsh, C. B., Shea, J. M. and Pomeroy, J. W.: Globally scalable alpine snow metrics, *Remote Sensing of Environment*, 213, 61–72, doi:10.1016/j.rse.2018.05.012, 2018.
- Wheater, H. S.: Water Security – science and management challenges, *Proceedings of the International Association of Hydrological Sciences*, 366, 23–30, doi:10.5194/piahs-366-23-2015, 2015.
- Winstral, A., Elder, K. and Davis, R. E.: Spatial snow modeling of wind-redistributed snow using terrain-based parameters, *Journal of Hydrometeorology*, 3, 524–538, doi:10.1175/1525-7541(2002)003<0524:ssmowr>2.0.co;2, 2002.
- Wood, E. F., Roundy, J. K., Troy, T. J., Beek, L. P. H. van, Bierkens, M. F. P., Blyth, E., Roo, A. de, Döll, P., Ek, M., Famiglietti, J., Gochis, D., Giesen, N. van de, Houser, P., Jaffé, P. R., Kollet, S., Lehner, B., Lettenmaier, D. P., Peters-Lidard, C., Sivapalan, M., Sheffield, J., Wade, A. and Whitehead, P.: Hyperresolution global land surface modeling: Meeting a grand challenge for monitoring Earth’s terrestrial water, *Water Resources Research*, 47, doi:10.1029/2010wr010090, 2011.
- Zhao, L. and Gray, D. M.: Estimating snowmelt infiltration into frozen soils, *Hydrological Processes*, 13, 1827–1842, doi:10.1002/(sici)1099-1085(199909)13:12/13<1827::aid-hyp896>3.0.co;2-d, 1999.